Historical Redlining and Disparities in Neighborhood Violence*

Steven Mello† Aaron Cho‡

January 28, 2026

Abstract

We use geocoded data on gun violence incidents to document disparities in exposure to neighborhood violence by race and income. We then explore the historical roots of these disparities, using a border discontinuity design approach to estimate the causal effect of "redlining" policies during the Great Depression on contemporary gun violence. The prevalence of gun violence changes sharply at borders associated with changes in creditworthiness designations in the 1930's. A decomposition exercise suggests that five percent of contemporary group disparities in exposure to neighborhood violence can be explained by the persistent effects of historical "redlining."

JEL Codes: K42, R23, J15, I14

*We are grateful to Elizabeth Cascio, Ingrid Ellen, Dan Fetter, Dan Hartley, Erzo Luttmer, Chris Snyder, and Doug Staiger for helpful feedback. Andrew Zuo provided helpful research assistance. We thank Sharon Williams for sharing the Gun Violence Archive data and Luca Perdoni for sharing his maps with predicted HOLC grades. Any errors are our own.

†Dartmouth College and NBER; steve.mello@dartmouth.edu.

‡Dartmouth College; aaron.k.cho@dartmouth.edu

1 Introduction

Violent crime is spatially concentrated, with a small share of neighborhoods typically accounting for a disproportionate share of violence (e.g., Weisburd 2015). Even beyond a heightened risk of victimization (Van Wilsem et al., 2006), exposure to neighborhood violence is associated with a host of adverse outcomes, including weaker academic performance and elevated cortisol levels among youth (Schwartz et al. 2022; Heissel et al. 2018), worse measures of mental and physical health (Dustmann & Fasani 2016; Baranyi et al. 2021; Khatana et al. 2022), and adverse employment outcomes for young men (Ihlanfeldt, 2006).

However, the lack of broad availability of data on violence at the neighborhood level has hampered efforts to understand the extent of and variation in exposure to violent neighborhoods in the United States. Moreover, little is known about the determinants of crime concentration and, over the long run, what factors create violent neighborhoods.

In this paper, we use novel data covering the near-universe of gun violence events in the U.S. since 2014 from the Gun Violence Archive (GVA) to measure disparities in exposure to neighborhood violence and study the historical roots of these disparities. Geocoding gun violence incidents to census tracts, we first compute disparities across salient race and income groups in exposure to neighborhood violence, defined as the annual number of gun violence incidents per 10,000 residents in the average tract inhabited by a member of a particular group. While statistics of this type can be computed at the county-level using CDC data on firearm fatalities or for select cities that provide geocoded crime data, we are the first (to our knowledge) to report these statistics at a sub-county level for the entire U.S.

We document striking disparities across race and income groups in exposure to gun violence. On average, Black and Hispanic individuals live in neighborhoods which are five and two times more violent than white individuals, respectively. Neighborhoods inhabited by typical households with incomes below $25,000 are about 60 percent more violent than those with incomes above $100,000. In the case of both race and income disparities, only about 20 percent of the overall disparity is between counties, with the remainder attributable to sorting *within* counties, highlighting the importance of our geocoded data for understanding group disparities in exposure to local violence.

We then study the historical roots of these disparities, focusing on differences in access to credit across neighborhoods resulting from Great Depression-era federal housing policy. During the 1930's, the Roosevelt administration established the Home Owner's Loan Corporation (HOLC) to refinance defaulted mortgages with the goal of stabilizing the distressed housing market. Beginning in 1936, the HOLC constructed maps of over 200 cities, known colloquially as "redlining" maps, which assigned letter grades to neighborhoods based on their creditworthiness.[1] While some have questioned the practical significance of HOLC des-

[1]Because the HOLC maps have received significant attention in the economics literature over the past ten years, we provide only this brief summary of the program here and defer interested

ignations (Fishback et al., 2024), others have contended that assigned grades had meaningful impacts on mortgage lending into the 1960's (Jackson, 1987). Recent empirical work has documented impacts of HOLC designations on neighborhood characteristics into at least the late twentieth century (e.g., Aaronson et al. 2021; Hynsjo & Perdoni 2024).

To estimate the persistent impact of HOLC grades on neighborhood violence, we use a border discontinuity design (e.g., Black 1999), studying how the prevalence of gun violence changes at HOLC borders associated with grade changes (e.g., areas graded as "A," which were deemed minimal risk for banks and areas graded as "D," considered hazardous for lenders). These borders have not had any explicit, legal significance since 1968, when the practice of "redlining" was banned by the Fair Housing Act (Federal Reserve History, 2023).

We implement our border discontinuity approach by aggregating the GVA data to the (2010) census block level and then geocoding block centroids to HOLC polygon borders. Our analysis sample is comprised of roughly 400,000 census blocks whose centroids are within 1,000 meters ($\approx$ 0.6 miles) of a HOLC polygon border. These blocks are drawn from 223 cities and account for about ten percent of the U.S. population as of the 2010 census.

Our border discontinuity estimates suggest large changes in gun violence at HOLC area borders. The probability of any gun violence incident (over 2014–2023) declines by 2.5 percentage points (about 20 percent) when crossing from the lower-graded to higher-graded side of the border. These changes are visually and statistically detectable even within very narrow windows (e.g., 200 meters) around HOLC borders. We find comparable effects when examining alternative measures of violence and our estimates are robust to dropping HOLC borders which overlap with "natural" boundaries, accounting for differential representation of blocks in our sample, and a host of alternative specification choices.

An important concern for the validity of our design is the worry that borders were drawn to coincide with sharp changes in neighborhood character even prior to the HOLC maps (Aaronson et al. 2021; Fishback et al. 2024). We speak to this concern in two ways. First, we show no long-run impacts on violence for a set of placebo borders which were drawn in the HOLC maps but were not associated with changes in HOLC grades. And second, we use an alternative research design which does not rely on border locations for identification. Building on Hynsjo & Perdoni (2024), this approach leverages the fact that only cities with at least 40,000 residents in 1930 were surveyed by the HOLC. We compare neighborhoods predicted to receive different grades based on their 1930 characteristics for cities just above and below the population threshold and attribute differential differences across predicted grades in mapped cities relative to unmapped cities to the HOLC maps. Estimated impacts of HOLC grades on violence from this alternative DiD approach are strikingly similar to those from our border discontinuity approach.

Accompanying our finding that historical HOLC grades influence present day violence, we find changes to other neighborhood characteristics at area borders: census blocks on

readers to dedicated sources such as Nelson et al. (2021) for further details.

the lower-graded sides of HOLC borders have higher minority population shares and lower median incomes in the 2010 ACS. Splitting our border discontinuity estimates by grade combinations, we find that borders associated with larger changes in neighborhood characteristics are also those associated with larger changes in the prevalence of violence, highlighting the impact of HOLC maps on neighborhood trajectories between the 1930's and the present day as an important mechanism for the estimated impacts on violence.

We conclude with a decomposition exercise asking to what extent contemporary group disparities in exposure to neighborhood violence can be explained by the persistent impacts of "redlining" suggested by our border discontinuity estimates. For bins at the level of a city $\times$ HOLC grade, we compute "causal counterfactual" estimates of gun violence and neighborhood composition which conservatively assume that HOLC designations affect only the spatial distribution of violence and group residences and impose that the relationship between HOLC grades and neighborhood characteristics match our causal estimates. While the large majority of present day disparities in violence exposure can be explained by sorting within city $\times$ neighborhoods with the same 1930's HOLC grades, we estimate that about five percent of present day race and income disparities in exposure to neighborhood violence can be explained by the persistent impacts of "redlining."

Our paper speaks to a broad literature in the social sciences on the historical persistence of public policy and economic or cultural phenomena (e.g., Acemoglu et al. 2001; Cirone & Pepinsky 2022; Nunn 2020), including several studies documenting the long-run impacts of historically significant borders (e.g., Dell 2010; Dell & Querubin 2018; Ambrus et al. 2020). More directly, our paper contributes to a rapidly growing literature on the legacy of segregation policies during the eary twentieth century generally (e.g., Faber 2020; Sood & Ehrman-Solberg 2024; Rothstein 2017) and specifically on the long-run impacts of the HOLC "redlining" maps on neighborhoods (e.g., Aaronson et al. 2021; Aaronson et al. 2021; Hynsjo & Perdoni 2024; Hoffman et al. 2020; Lynch et al. 2021).

A smaller literature has also considered the relationship between "redlining" and crime. Winslow et al. (2025) document correlations between historical HOLC grades and present day levels of violence. Anders (2023) finds higher contemporary crime rates in cities that were "redlined" than those that were not, leveraging the 1930's population threshold for HOLC mapping for identification. Poulson et al. (2023) show increases in violence at borders between A- and D- graded HOLC areas in Boston. Our contribution relative to the existing literature on this topic is twofold. First, we provide quasi-experimental RD evidence on the persistent impact of HOLC maps for all (mapped) cities and grade combinations. And second, we contextualize our estimated persistence effects with our novel descriptive evidence on present day group disparities in exposure to neighborhood violence.

Our findings also contribute to a vast literature on disadvantaged neighborhoods (e.g., Wilson 1987; Chyn & Katz 2021) and the relationship between residential segregation and the conditions of urban areas. Prior studies have documented that more segregated cities are

poorer (Ananat, 2011) and have lower levels of upward mobility (Chetty et al., 2018), as well as highlighted segregation as a driver of racial disparities in health outcomes (Williams & Collins, 2001), educational achievement (Reardon et al., 2022); and homicide victimization (Cox et al., 2025). We provide novel descriptive evidence on the role of residential segregation in explaining variation across race and income groups in exposure to neighborhood violence and new causal evidence on the persistence of historical segregation policies in determining which neighborhoods are most violent nearly a century later.

The remainder of our paper proceeds as follows. Section 2 describes the data and summarizes present day disparities in exposure to neighborhood violence. Section 3 lays out our empirical strategy for estimating the impacts of historical HOLC designations and section 4 presents the associated results. We conclude by discussing our findings in the context of present day disparities in section 5.

2 Data and descriptive statistics

2.1 Gun violence data

Data on gun violence incidents from 2014–2023 was provided by the Gun Violence Archive ("GVA"), which collects and compiles incident-level records of shootings associated with a fatality or injury with the goal of constructing a database covering all gun violence in the United States. According to their website, the GVA collects data via "automated queries [and] manual research through over 7,500 sources from local and state police, media, data aggregators, government and other sources daily. Each event is verified by both researches and a secondary validation process."

For our purposes, the key feature of the GVA data is that it provides GPS coordinates associated with each incident. In our analyses, we geocode GVA incidents into census blocks and construct four primary measures of violence exposure for various geographies: (i) an indicator for whether any gun violence incident occurred, 2014–2023; (ii) the number of incidents, 2014–2023; (iii) the annualized number of incidents per 10,000 residents; (iv) the annualized number of incidents per square KM.[2]

There are, of course, natural questions about the validity and coverage of the GVA data. In a recent examination, Gobaudet al. (2023) find that the GVA data include about 80 percent of shootings reported in official police department records for four large and medium-sized cities. We provide two additional validation exercises in appendix E-1. First, we show that the GVA data on gun fatalities closely tracks the comparable CDC data at the state-year level. Second, we document a strong correlation between levels of violence in the GVA

[2]Annualized measures divide the total count of units by 9, the number of years in our GVA data, and then by either number of residents/10,000 or by area. We consider alternative outcomes based on the reported number of injuries or fatalities in table B-4.

data and overall crime at the census tract level within cities for 13 cities which publish crime data with GPS coordinates. Importantly, for our border discontinuity analysis, we need only to assume that coverage of the GVA data does not change discretely at HOLC neighborhood boundaries within cities.

Although largely unused in the economics literature, the GVA data has been used in the sociology, epidemiology, and public health literatures to study, for example, youth exposure to gun violence in select U.S. cities (Kravitz-Wirtz et al., 2022) and effects of proximate gun violence on youth outcomes (e.g., Gard et al. 2022; Buggset al. 2022).

2.2 Other data sources

For both our descriptive and border discontinuity analyses, we rely on data on neighborhood characteristics from the 2010 decennial census and the 2010 American Community Survey, as well as maps of various census geographies from the Census Bureau. Note that, in our border discontinuity analysis, the unit of analysis is a census block. We can directly measure a block's racial composition using information the 2010 decennial census, but other neighborhood characteristics of interest from the ACS are only observed at the block group level. For these measures, we assign each block the value associated with its block group.

Our data on 1930's HOLC "redlining" maps are from Nelson et al. (2021), who provide maps in GIS format through the University of Richmond. These maps indicate polygons corresponding to each "neighborhood" (polyon) delineated by the HOLC and provide the associate HOLC grade (A, B, C, D). For our border discontinuity analysis, we geocode 2010 census block centroids into HOLC area polygons. We also construct line segments corresponding to the shared border of each adjacent polygon ("border segments"), as described in appendix E-2, and then compute distances from each census block centroid and all border segments associated with the HOLC polygon in which that census block centroid lies.

In our descriptive analysis of census tracts below, we report statistics for both all tracts in the U.S. and for the subset of tracts corresponding to areas that were mapped by the HOLC. We consider a tract to be a HOLC tract if the centroid of any census block lying within that tract is geocoded to a HOLC polygon. Our HOLC sample is comprised of 223 cities, with the geographic representation of this sample depicted in figure A-3.

2.3 Descriptive analysis

We first use the GVA data to quantify differences across groups in exposure to neighborhood violence. For census tract j, we compute the following measure of neighborhood violence:

$$v_j = \frac{annual\ incidents_j}{residents_j/10,000}$$

For some group g, average neighborhood-level exposure can then be computed as:

$$\bar{v}_g = \sum_j \omega_{gj} v_j,$$

where $\omega_{gj} = Pr(j_i = j|G = g)$. In other words, $\bar{v}_g$ is a weighted average of the neighborhood-level v_j's, with weights equal to the share of group g residing in neighborhood j, and can be interpreted as the level of violence in the average neighborhood inhabited by an individual from group g. Note that neighborhood-level violence v_j is not group-specific; differences across groups in $\bar{v}_g$ are due only to differences across groups in neighborhoods of residence.

Figure 1 depicts differences in exposure to neighborhood violence by race and household income in the U.S. In each panel, we report $\bar{v}_g$ using all census tracts ($N = 73,057$) and census tracts in HOLC areas ($N = 15,018$), as well as overall and within-county differences. Differences across racial groups, shown in panel (a), are especially striking. Relative to the average white individual, average Black and Hispanic individuals live in neighborhoods which are five and two times more violent, respectively. Proportionally, racial disparities are similar in the subset of HOLC tracts, which exhibit higher levels of violence on average (unsurprisingly given that these are primarily urban areas).

We also document stark differences by household income in panel (b). Households with annual incomes below $25,000 live in neighborhoods which are roughly 60 percent more violent than households with incomes above $100,000. As with race, disparities across income groups are proportionally similar for the subset of HOLC tracts.[3]

Highlighting the importance of focusing on local segregation patterns (and thus stressing the importance of the geocoded data on gun violence incidents for this exercise), both panels of figure 1 suggest a relatively small role for between-county variation. For example, only about 20-30 percent of the aggregate Black-white disparity in gun violence exposure can be explained by county-level variation, with the remainder attributable to variation across neighborhoods *within* counties.

To preview our analysis of historical "redlining", figure A-2 depicts the relationship between a census tract's 1930's HOLC grade and contemporary gun violence, as well as other neighborhood characteristics from the 2010 census. Higher HOLC grades are descriptively associated with statistically significant declines in gun violence, as well as declines in minority population shares and poverty rates.

[3]One might also be interested in racial disparities conditional on income (and vice versa). While the ACS does not report counts at the race *and* income group level for census tracts, counts by race *and* poverty status are available. In table A-2, we present comparable estimates to those presented in figure 1 for race × poverty status.

3 Empirical strategy

To assess the causal effect of HOLC grades on present day gun violence, we use a border discontinuity design (e.g., Black 1999) to study how violence changes around borders associated with HOLC grade changes.

For our border discontinuity design, we aggregate gun violence incidents to the (2010) census block-level. Implementation of the border design requires a unit of aggregation, and we choose census blocks for two reasons: (i) on average, many blocks fall within each HOLC polygon;[4] (ii) it is straightforward to assign measures of other neighborhood characteristics to census blocks, including racial composition (available directly at the census block level in the ACS), poverty rates, and median household incomes (available at the census block group-level in the ACS).[5]

We then use block centroids to assign blocks to HOLC polygons and to compute the distance between each block and all border segments associated with that block's designated HOLC polygon. This process yields a dataset which is at the block × border level, which each block copied once for each border segment associated with that block's designated HOLC polygon. We further trim this dataset to include only borders associated with a HOLC grade change and only blocks within 1,000 meters (≈ 0.6 miles) of the border.

Our goal is then to estimate regression models of the form:

$$Y_{ib} = \theta High_{ib} + f(\Delta_{ib}) + X_i + \epsilon_{ib} \tag{1}$$

where i indexes census blocks and b indexes borders, $High_{ib}$ is an indicator for whether block i falls on the higher graded side of border b, and Δ_{ib} is the distance between block i's centroid and border b, normalized so that positive (negative) distances correspond to the higher (lower) graded side of the border.

Importantly, because census blocks do not fall strictly within HOLC polygons, blocks whose centroids are very close to borders may fall partly within multiple polygons, eroding the discontinuity in treatment status at the border. We depict this point in panels (a) and (b) of figure B-2. Panel (a) depicts a sharp decline in the share of a block's area lying within its designated HOLC polygon among blocks very close to the border. Panel (b) shows a block's "GPA," defined as the area-weighted average HOLC grade for each block, as a function of normalized distance. By construction, blocks lying mostly within neighboring HOLC areas of different grades exhibit large GPA differences. However, because blocks which are very close to borders tend to lie within multiple areas, the discontinuity in this area-weighted

[4] In HOLC graded cities, the average census block is 0.2 KM^2 and the median HOLC polygon is comprised of roughly 33 census blocks.

[5] Alternatively, rather than choosing a level of aggregation, one could compute the distance between incidents and HOLC borders and study the associated density. Figure B-1 illustrate results from this approach.

GPA right at the boundary is significantly attenuated.

To deal with this issue, we use a "donut" RD approach, dropping blocks whose centroids lie within a narrow window of borders. As our baseline approach, we set the donut to be $\sqrt{\bar{a}/\pi} = 81.2$ meters, where $\bar{a}$ is the average land area among graded census blocks. We retain this donut throughout our main analysis and report robustness to varying the choice of donut in figure B-5. Our donut RD analysis sample is made up of 720,840 block × border observations, with 8,801 unique HOLC borders and 402,024 unique census blocks, accounting for about 10 percent of the U.S. population as of 2010. Table A-4 reports summary statistics for blocks in our analysis sample, as well as all blocks in the nation and blocks located in HOLC areas for comparison.

Using this donut blocks × borders sample, we obtain regression discontinuity estimates via two approaches: a linear specification of equation (1) and the robust, local polynomial approach from Calonico et al. (2014). Unless otherwise noted, linear specifications always use a bandwidth of 1,000 meters and local polynomial specifications use the Calonico et al. (2014) optimal bandwidth. As our baseline specification, we include city fixed effects and border type (i.e., grade combination) fixed effects. For linear specifications, we report standard errors which are two way-clustered at the border and block-level and for the local polynomial specifications, we cluster standard errors at the city-level.

To identify causal effects of historical HOLC designations on modern violence, our approach depends on the assumption that pre-HOLC neighborhood characteristics influencing long-run violence did not change discontinuously at boundaries. An important concern for our approach, then, is that borders were not drawn randomly (e.g., Rothstein 2017) and may have coincided with notable changes in the physical or demographic makeup of a neighborhood (e.g., Fishback et al. 2024). Note that while Aaronson et al. (2021) document that resident characteristics change with HOLC grades in a narrow (∼350m) buffer around borders in the 1930 census, these changes are not discontinuous exactly at HOLC borders and thus do not necessarily invalidate our boundary design.

Nonetheless, we speak to these concerns in two additional ways. Firstly, we repeat our analysis using a set of placebo borders. Specifically, we construct a secondary blocks × border dataset which is identical to our analysis sample except for borders *without* grade changes (e.g., borders between two C-graded polygons). We then assign placebo higher and lower grade designations among bordering polygons based on the average grades of their adjacent polygons and repeat our analysis using this alternative sample of borders without a grade change.[6] And second, we present estimates from an alternative research design building on Hynsjo & Perdoni (2024) which does not exploit the location HOLC borders

[6]For example, imagine two adjacent polygons denoted P_1 and P_2 with identical grades. Suppose that P_1 borders polygons P_2, P_3, and P_4, while P_2 borders polygons P_1, P_5, and P_6. If the average grade among polygons P_3 and P_4 is higher than the average grade among polygons P_5 and P_6, we designate P_1 as the higher graded polygon in the placebo $\{P_1, P_2\}$ pair.

and explicitly controls for pre-existing differences in characteristics between areas graded differently, described further below in section 4.1 and appendix C.

4 Results

Figure 2 depicts our baseline border discontinuity estimates. In panel (a), we depict the implicit first stage underlying our approach, illustrating the change in HOLC grades at the boundary. Note that, in order to quantify this first stage relationship, we convert HOLC letter grades into a standard GPA scale (A = 4, B = 3, and so on). The horizontal axis indicates the distance of a block's centroid from the border, with negative (positive) values indicating that a block falls on the lower (higher) graded side of the border.

In our analysis sample of grade change borders, shown with blue circles, there is a sharp increase of about 1.1 grade points when crossing the border.[7] There is no such change for our set of placebo borders without a grade change. Both these relationships are by construction.

Panel (b), which depicts our main result, is identical to panel (a) except that the outcome of interest is an indicator whether a block experienced any gun violence incidents during 2014–2023. Around borders with a grade change (again depicted in blue circles), we observe a sharp decline in the likelihood of gun violence when moving from the lower- to higher-graded side of the border. The corresponding linear RD estimate is -0.025 ($se = 0.002$), which represents roughly a 20 percent decline relative to the average prevalence of violence among blocks on the lower-graded side of the border.

Note that there is no such discrete change in gun violence at placebo borders (again depicted with gray squares) between HOLC polygons given the same grade, and the associated linear RD coefficient is a precisely estimated null effect.

4.1 Robustness

Table 1 presents border discontinuity estimates for four measures of block-level gun violence: the number of incidents during 2014–2023, any incident during 2014–2023, annualized incidents per 10,000 residents, and annualized incidents per KM^2. In the table, we present estimates for four different specifications using both the linear approach and local polynomial approach from Calonico et al. (2014). The estimate in the first row, column (2), corresponds to that reported in figure 2.

To account for the fact that our baseline sample includes multiple observations per census block, the second and sixth rows report estimates which reweight census blocks by the inverse of their number of observations in our baseline blocks × border sample. To address

[7] Note that the fact that this RD estimate is close to one implies that the majority of our sample is comprised of borders where adjacent polygons are one grade apart. We report the distribution of grade combinations in our baseline sample in table B-6.

the concern that HOLC boundaries coincide with natural borders that may have independently impacted the evolution of neighborhood characteristics, rows three and seven report estimates which drop borders overlapping with rivers and railroad tracks, following Aaronson et al. (2021).[8] The fourth and eighth rows report estimates which both drop these "natural" borders and downweight census blocks.

Within linear or local polynomial estimation approaches, these alternative specifications have only minimal implications for the border discontinuity estimates. When examining incident counts or the binary outcome measure (columns 1 and 2), estimates using the local polynomial approach are attenuated relative to the baseline approach, in some cases by nearly half, but estimates from the more demanding local polynomial specifications are still statistically significant at conventional levels and represent meaningful changes at the border, roughly ten percent declines relative to the mean on the lower-graded side. Estimates using scaled outcome measures (columns 3 and 4) are similar across estimation approaches.

In appendix B, we report results from additional robustness tests, including results for alternative violence outcomes (table B-4), estimates when varying the choice of fixed effects (table B-3), and estimates when varying the choice of donut or bandwidth size (figure B-5).

We also compute estimates using an alternative research design which does not exploit the location of HOLC borders in appendix C. This approach builds on Hynsjo & Perdoni (2024), who leverage the fact that only sufficiently large cities ($\geq$ 40,000 residents in 1930) were mapped by the HOLC and compare outcomes for neighborhoods, defined as neutrally drawn hexagons of roughly 0.25 KM^2, predicted to receive the same HOLC grade based on pre-HOLC characteristics in cities above and below this population threshold.

Using 97 cities with populations between 30,000 and 60,000 in the 1930 census, we implement a cross-sectional DiD version of their strategy which compares the prevalence of violence in areas predicted to receive different HOLC grades in cities above and below the population threshold. For example, we compare present day violence in neighborhoods predicted to receive grades of B and C in cities which were and were not mapped and attribute additional differences between B and C areas in mapped cities, relative to those that were not actually mapped, to the HOLC maps. Aggregating across grade combinations for comparability with our border discontinuity estimates, we find strikingly similar estimated impacts of HOLC grades on violence from this alternative strategy, as shown in appendix C.

4.2 Comparison with OLS

A natural question is how our border discontinuity estimates of the impact of HOLC grades compare to observational (non-causal) estimates. In tables B-1 and B-2, we report OLS

[8] See appendix E-3 for additional details on our definition of natural boundaries. We use a very conservative notion based on whether there is a railroad or river within 200 meters of a border. Our donut RD sample when dropping these boundaries is comprised of 325,599 blocks $\times$ borders (214,029 unique blocks and 4,400 unique borders).

estimates which are directly comparable to our border discontinuity estimates. These are constructed by estimating regressions of a given outcome on HOLC grade indicators and city fixed effects using the set of blocks including in our analysis sample, constructing grade increase effects for each grade combination, and then averaging, weighting by each grade combinations's representation in our analysis sample.

For gun violence outcomes, our donut RD estimates are generally 30–40 percent as large as the comparable OLS estimates, suggesting that while historical HOLC designations are important determinants of present day violence, observational comparisons across HOLC areas are biased away from zero by omitted variables.

4.3 Grade-specific results

While our baseline estimates pool together all borders with a grade change, we report estimates for specific border types (i.e., grade combinations) in figure 3. Specifically, first we estimate border discontinuities separately for each grade combination using our baseline approach. We then plot the border type-specific RD estimate for gun violence (vertical axis) against the corresponding estimate for neighborhood characteristics as of the 2010 American Community Survey (horizontal axis).[9]

We find that border types with the largest long-run impacts on neighborhood characteristics are also those with the largest long-run impacts on violence. Borders between A- and D-graded polygons are associated with the largest changes in both neighborhood characteristics and violence, but these estimates are imprecise, as A–D borders account for just one percent of our sample (see table B-6).

One could think of figure 3 as type of mechanisms analysis, plotting the relationship between our instrument (HOLC borders) and outcome on the vertical axis against the relationship between the instrument and a "mediator" on the horizontal axis. Viewed through this lens, figure 3 highlights the impact of HOLC grades on the evolution of neighborhoods in the years between the 1930's and present day, possibly both in terms of social structure (e.g., Aaronson et al. 2021) and the physical environment (e.g., Ellen et al. 2013), as an important mechanism for explaining differences in contemporary violence.

5 Discussion

We conclude by marrying together the descriptive findings from section 2 with the border discontinuity estimates from section 4. Specifically, we ask to what extent the persistent effects of "redlining" can explain group disparities in exposure to neighborhood violence. Using the same notation as in section 2, denote the difference in violence exposure across

[9]Border discontinuity estimates for neighborhood characteristics using our full blocks × borders analysis sample are presented in figure B-4 and table B-5.

groups g, h by:

$$\Delta_{g,h} = \bar{v}_g - \bar{v}_h = \sum_j \omega_{gj} v_j - \sum_j \omega_{hj} v_j = \sum_j (\omega_{gj} - \omega_{hj}) v_j$$

Our goal is then to decompose $\Delta_{g,h}$. Each tract j lies within a city c and is assigned a modal HOLC grade, and let q denote cells defined by the combination of city and grade. $\Delta_{g,h}$ can then be rewritten as:

$$\Delta_{g,h} = \underbrace{\sum_c (\omega_{gc} - \omega_{hc}) v_c}_{\text{sorting between cities}} + \underbrace{\sum_j (\omega_{gj} - \omega_{hj})(v_j - v_{q(j)})}_{\text{sorting within cities} \times \text{grades}} + \underbrace{\sum_q (\omega_{gq} - \omega_{hq})(v_q - v_{c(q)})}_{\text{sorting between grades within cities}}$$

where $v_{q(j)}$ and $v_{c(j)}$ are the cell- and city-level average violence for the cell and city containing tract j, respectively. The first term captures between-city differences (e.g., the propensity of certain groups to live in higher violence cities) while the second term captures sorting within city $\times$ HOLC grades (e.g., the propensity of certain groups to live in more violent neighborhoods even among those with the same historical HOLC designations).

The last term above can be further decomposed into:

$$\begin{aligned}
\sum_q (\omega_{gq} - \omega_{hq})(v_q - v_{c(q)}) = & \underbrace{\sum_q (\omega_{gq} - \omega_{hq}) \Big[(v_q - v_{c(q)}) - (\tilde{v}_q - v_{c(q)}) \Big]}_{\text{within-}c\text{ outcome effect } (\equiv \Delta^{\tilde{v}}_{g,h})} \\
& + \underbrace{\sum_q \Big[(\omega_{gq} - \omega_{hq}) - (\tilde{\omega}_{gq} - \tilde{\omega}_{hq}) \Big] \big(\tilde{v}_q - v_{c(q)} \big)}_{\text{within-}c\text{ reweighting effect } (\equiv \Delta^{\tilde{\omega}}_{g,h})} \\
& + \underbrace{\sum_q (\tilde{\omega}_{gq} - \tilde{\omega}_{hq}) \big(\tilde{v}_q - v_{c(q)} \big)}_{\text{within-}c\text{ causal disparity } (\equiv \tilde{\Delta}_{g,h})},
\end{aligned}$$

where $\tilde{v}_q$, $\tilde{\omega}_{gq}$ and $\tilde{\omega}_{hq}$ are "causal counterfactuals" reflecting only the estimated causal relationship(s) between HOLC designations and neighborhood characteristics based on our border discontinuity design. To be conservative, we estimate these quantities under the assumption that HOLC grades impact only the spatial distribution of violence and residents of certain groups but not the levels. Our estimate of $\tilde{v}_q$ holds the total amount of violence in a given city c constant but imposes that the relationship between violence v and HOLC grades matches our RD estimates. Similarly, our estimates of $\tilde{\omega}_{gq}$ and $\tilde{\omega}_{hq}$ hold constant city-level population shares in groups g and h but match the relationship between neighborhood composition and HOLC grades with the associated RD estimates. For additional details on the estimation of these casual counterfactual terms, see appendix D.

The final term ($\tilde{\Delta}_{g,h}$), the causal counterfactual version of the original $\Delta_{g,h}$, measures the disparity in violence exposure implied only by the estimated impacts of HOLC grades on neighborhood violence and group composition, taking all observed between-city and within-city $\times$ grade sorting as given. For simplicity, it is useful to think of the other two terms, $\Delta^{\tilde{\omega}}_{g,h}$ and $\Delta^{\tilde{v}}_{g,h}$, as capturing residual sorting which is within-city and across HOLC grades.[10]

While this decomposition is conservative in the sense that it takes observed sorting between cities and sorting within city $\times$ grades as given, as well as assumes that estimates treatment effects are purely distributional, there is one important caveat worth highlighting. Specifically, this decomposition effectively assumes the causal effects of HOLC grading on neighborhood violence and neighborhood group composition to be independent.

Table 2 reports the results of this decomposition for exposure disparities between Black and Hispanic ("minority") individuals and white individuals and for households above and below the poverty line. In both cases, about 80 percent of the total disparity $\Delta_{g,h}$ is explained by sorting between-cities and sorting within city $\times$ grades, with a meaningful majority attributable to the latter component.

Nonetheless, we find a meaningful contribution of the causal effect of HOLC grades in both cases, with the causal counterfactual component ($\tilde{\Delta}_{g,h}$) explaining about 8 percent of the overall minority-white disparity and 5 percent of the overall above-below poverty line disparity. Both estimates are statistically significant at conventional levels. Focusing only on the within-city, between-grade disparities which is allowed to be explained by HOLC treatment effects (by assumption), the purely causal component can explain about 40 (25) percent in the case of the minority versus white (poor versus non-poor) disparity.

The central takeaway from this decomposition exercise is that the persistent effects of "redlining" are sufficiently large to be quantitatively relevant for understanding contemporary disparities across groups in exposure to neighborhood violence. We estimate that 5-8 percent of present day race and income disparities in exposure to neighborhood gun violence can be explained by the persistent impacts of "redlining" on the spatial distribution of violence and neighborhoods of residents across salient groups.

[10] A well-known feature of Oaxaca-Blinder style decompositions is that they are not unique (e.g., Neumark 1988). In particular, the ordering of the first two terms in the decomposition of within-c between-grade sorting term is relevant for the associated magnitudes.

References

Aaronson, D., Faber, J. W., Hartley, D., Mazumder, B., & Sharkey, P. (2021). The long-run effects of the 1930s holc "redlining" maps on place-based measures of economic opportunity and socioeconomic success. *Regional Science and Urban Economics*, *86*, 103622.

Aaronson, D., Hartley, D., & Mazumder, B. (2021). The effects of the 1930s holc "redlining" maps. *American Economic Journal: Economic Policy*, *13*(4), 355–392.

Acemoglu, D., Johnson, S., & Robinson, J. A. (2001). The colonial origins of comparative development: An empirical investigation. *American Economic Review*, *91*(5), 1369–1401.

Ambrus, A., Field, E., & Gonzalez, R. (2020). Loss in the time of cholera: Long-run impact of a disease epidemic on the urban landscape. *American Economic Review*, *110*(2), 475–525.

Ananat, E. O. (2011). The wrong side(s) of the tracks: The causal effects of racial segregation on urban poverty and inequality. *American Economic Journal: Applied Economics*, *3*(2), 34–66. Acute causal estimates of segregation using historical railroad placement as an instrument.

Anders, J. (2023). The long run effects of de jure discrimination in the credit market: How redlining increased crime. *Journal of Public Economics*, *222*, 104857.

Atack, J. (2016). Historical geographic information systems (gis) database of u.s. railroads for 1826–1911. Computer file. May 2016; revised 2022.

Baranyi, G., Di Marco, M. H., Russ, T. C., Dibben, C., & Pearce, J. (2021). The impact of neighbourhood crime on mental health: a systematic review and meta-analysis. *Social Science & Medicine*, *282*, 114106.

Black, S. E. (1999). Do better schools matter? parental valuation of elementary education. *Quarterly Journal of Economics*, *114*(2), 577–599.

Buggs, S. A. L. et al. (2022). Heterogeneous effects of spatially proximate firearm violence exposure on youth outcomes. *Preventive Medicine (Author manuscript)*. GVA data linked to Fragile Families and Child Wellbeing Study to construct exposure measures.

Calonico, S., Cattaneo, M. D., & Titiunik, R. (2014). Robust nonparametric confidence intervals for regression-discontinuity designs. *Econometrica*, *82*(6), 2295–2326.

Chetty, R., Friedman, J. N., Hendren, N., Jones, M. R., & Porter, S. R. (2018). The opportunity atlas: Mapping the childhood roots of social mobility. Online data product and research project, Opportunity Insights. Available at https://opportunityatlas.org; accessed January 6, 2026.

Chyn, E. & Katz, L. F. (2021). Neighborhoods matter: Assessing the evidence for place effects. *Journal of Economic Perspectives*, *35*(4), 197–222.

Cirone, A. & Pepinsky, T. B. (2022). Historical persistence. *Annual Review of Political Science*, *25*, 241–259.

Cox, R., Cunningham, J. P., Ortega, A., & Whaley, K. D. (2025). Black lives: The high cost of segregation. *American Economic Journal: Economic Policy*. Forthcoming.

Dell, M. (2010). The persistent effects of peru's mining *mita*. *Econometrica*, *78*(6), 1863–1903.

Dell, M. & Querubin, P. (2018). Nation building through foreign intervention: Evidence from discontinuities in military strategies. *The Quarterly Journal of Economics*, *133*(2), 701–764.

Dustmann, C. & Fasani, F. (2016). The effect of local area crime on mental health. *Economic Journal*, *126*(593), 978–1017.

Ellen, I. G., Lacoe, J., & Sharygin, C. A. (2013). Do foreclosures cause crime? *Journal of Urban Economics*, *74*, 59–70.

Faber, J. W. (2020). We built this: Consequences of new deal era intervention in america's racial geography. *American Sociological Review*, *85*(6), 739–775.

Federal Reserve History (2023). Redlining. Federal Reserve History, an online essay. Published June 2, 2023; accessed January 6, 2026.

Fishback, P. V., Rose, J., Snowden, K. A., & Storrs, T. (2024). New evidence on redlining by federal housing programs in the 1930s. *Journal of Urban Economics*, *141*, 1034–62.

Gard, A. M., Brooks-Gunn, J., McLanahan, S. S., Mitchell, C., Monk, C. S., & Hyde, L. W. (2022). Deadly gun violence, neighborhood collective efficacy, and adolescent neurobehavioral outcomes. *PNAS Nexus*, *1*(3), pgac061.

Gobaud, A. N. et al. (2023). Assessing the gun violence archive as an epidemiologic data source. *JAMA Network Open*.

Heissel, J. A., Sharkey, P. T., Torrats-Espinosa, G., Grant, K. E., & Adam, E. K. (2018). Violence and vigilance: The acute effects of community violent crime on sleep and cortisol. *Child Development*, *89*(4), e323–e331.

Hoffman, J. S., Shandas, V., & Pendleton, N. (2020). The effects of historical housing policies on resident exposure to intra-urban heat: A study of 108 us urban areas. *Climate*, *8*(1), 12.

Hynsjo, D. & Perdoni, L. (2024). Mapping out institutional discrimination: The economic effects of federal redlining. Available at SSRN; doi:10.2139/ssrn.4820845.

Ihlanfeldt, K. R. (2006). Neighborhood crime and young males' job opportunity. *Journal of Law and Economics*, *49*(1), 249–283.

Jackson, K. T. (1987). *Crabgrass Frontier: The Suburbanization of the United States*. New York: Oxford University Press.

Khatana, S. S., Goyal, A., Gottesman, R. F., et al. (2022). Association between community-level violent crime and cardiovascular mortality rates in chicago, 2000–2014. *Journal of the American Heart Association*, *11*(1), e025168. Longitudinal community-area panel study linking violent crime exposure to cardiovascular mortality in Chicago.

Kravitz-Wirtz, N., Bruns, A., Aubel, A. J., Zhang, X., & Buggs, S. A. (2022). Inequities in community exposure to deadly gun violence by race/ethnicity, poverty, and neighborhood disadvantage among youth in large u.s. cities. *Journal of Urban Health*, *99*(4), 610625.

Lynch, E. E., Malcoe, L. H., Laurent, S. E., Richardson, J., Mitchell, B. C., & Meier, H. C. S. (2021). The legacy of structural racism: Associations between historic redlining, current mortgage lending, and health. *SSM Population Health*, *14*, 100793.

McCrary, J. (2008). Manipulation of the running variable in the regression discontinuity design: A density test. *Journal of Econometrics*, *142*(2), 698–714.

Nelson, R. K., Winling, L., Marciano, R., Connolly, N., & et al. (2021). Mapping inequality. American Panorama, Digital Scholarship Lab. Accessed December 15, 2016.

Neumark, D. (1988). Employers' discriminatory behavior and the estimation of wage discrimination. *The Journal of Human Resources*, *23*(3), 279–295.

Nunn, N. (2020). The historical roots of economic development. *Science*, *367*(6485), eaaz9986.

Pebesma, E. (2018). Simple features for r: Standardized support for spatial vector data. *The R Journal*, *10*(1), 439–446.

Poulson, M. R., Neufeld, M. Y., LaRaja, A., Allee, L., Kenzik, K. M., & Dechert, T. (2023). The effect of historic redlining on firearm violence. *Journal of the National Medical Association*, *115*(9), 421–427.

Reardon, S. F., Weathers, E. S., Fahle, E. M., Jang, H., & Kalogrides, D. (2022). Is separate still unequal? new evidence on school segregation and racial academic achievement gaps. CEPA Working Paper 19-06, Stanford Center for Education Policy Analysis (CEPA).

Rothstein, R. (2017). *The Color of Law: A Forgotten History of How Our Government Segregated America* (1st ed.). New York & London: Liveright Publishing Corporation (a division of W.W. Norton & Company).

Schwartz, A. E., Laurito, A., Lacoe, J., Sharkey, P., & Ellen, I. G. (2022). The academic effects of chronic exposure to neighbourhood violence. *Urban Studies*, *59*(14), 3005–3021.

Sood, A. & Ehrman-Solberg, K. (2024). The long shadow of housing discrimination: Evidence from racial covenants. SSRN Working Paper.

Van Wilsem, J., Wittebrood, K., & De Graaf, N. D. (2006). Socioeconomic dynamics of neighborhoods and the risk of crime victimization: A multilevel study of improving, declining, and stable areas in the netherlands. *Social Problems*, *53*(2), 226–247.

Weisburd, D. (2015). The law of crime concentration and the criminology of place. *Criminology*, *53*(2), 133–157.

Williams, D. R. & Collins, C. (2001). Racial residential segregation: a fundamental cause of racial disparities in health. *Public Health Reports*, *116*(5), 404–416.

Wilson, W. J. (1987). *The Truly Disadvantaged: The Inner City, the Underclass, and Public Policy*. Chicago, IL: University of Chicago Press.

Winslow, K. R., Wurdeman, T. D., Ordoobadi, A. J., Jarman, M. P., & Anderson, G. A. (2025). Strong laws aren't enough: Historic redlining, state firearm laws, and urban firearm violence in the united states. *The American Journal of Surgery*, *251*, 116537.

Figure 1: Exposure to neighborhood (census tract) gun violence by group

(a) Race

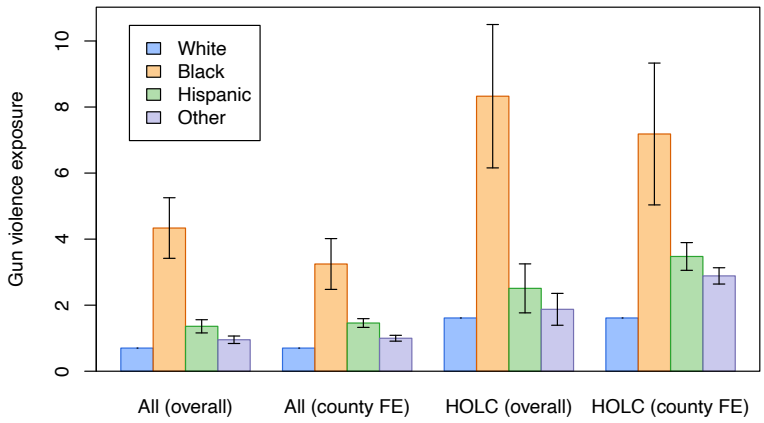

(b) Household income

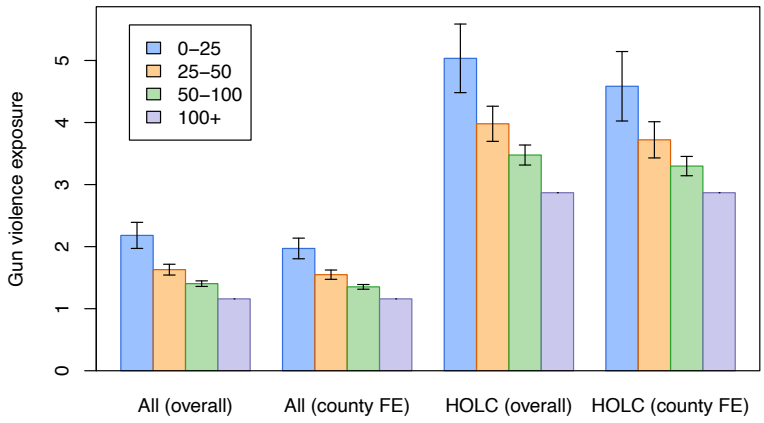

*N*otes: This figure depicts average gun violence exposure, defined as the annual number of gun violence incidents per 10,000 population in the census tract of residence, for different groups. In each panel, we report overall and within-county exposure using all tracts in the U.S. and only those tracts in HOLC areas. Confidence bands are 95 percent confidence bands, constructed from standard errors clustered at the county-level, from regressions comparing exposure across groups relative to a reference group (white in panel a, income $\geq$ \$100,000 in panel b). These regression estimates are presented in table A-1.

Figure 2: Border discontinuity estimates

(a) HOLC grade (1930's)

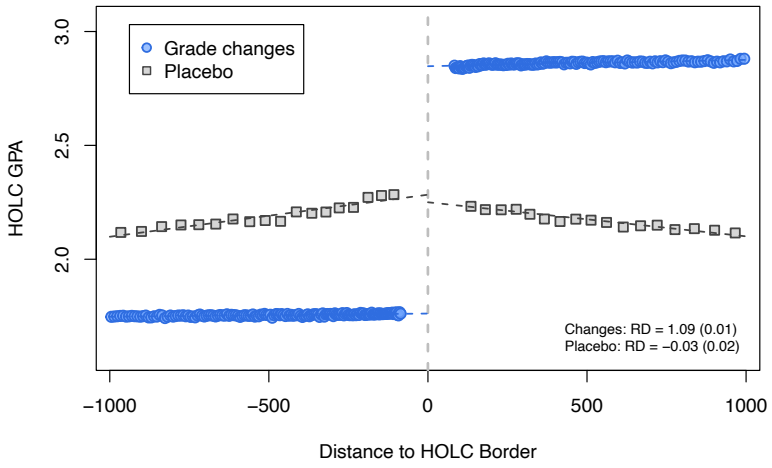

(b) Any gun violence incident (2014-2023)

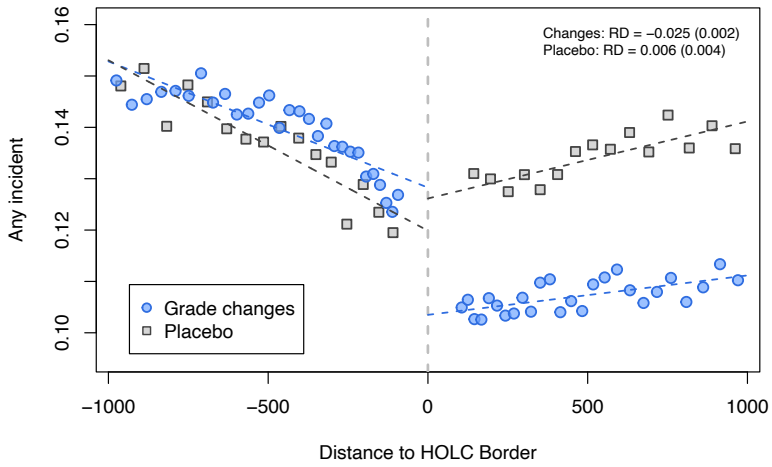

*N*otes: Each panel depicts a binscatter plot of the relationship between a census block's distance from a HOLC polygon border (horizontal axis) and the denoted outcome (vertical axis). In panel (a), the outcome is a census block's HOLC GPA and in panel (b), the outcome is whether there was any gun violence incident in a census block over 2014−2023. Blue circles correspond to our baseline donut RD sample around borders associated with a grade change. Gray squares correspond to our placebo donut RD sample around borders without a grade change ($N = 307,865$ blocks $\times$ borders; 217,476 unique census blocks; 3,986 unique borders).

Table 1: Donut RD estimates, impact of HOLC grade increases

	(1) Incidents	(2) Any incident	(3) Incidents per 10,000	(4) Incidents per KM^2
Linear estimates				
Baseline	-0.046	-0.0248	-1.927	-0.351
	(0.006)	(0.0024)	(0.382)	(0.064)
Block-reweighted	-0.04	-0.0192	-1.712	-0.286
	(0.006)	(0.0022)	(0.43)	(0.062)
Drop rivers and rails	-0.059	-0.0297	-1.845	-0.481
	(0.007)	(0.0033)	(0.512)	(0.074)
Drop and reweighted	-0.048	-0.0228	-1.519	-0.346
	(0.008)	(0.0031)	(0.598)	(0.077)
Local polynomial estimates				
Baseline	-0.038	-0.0158	-2.134	-0.327
	(0.011)	(0.004)	(0.751)	(0.141)
	[0.0008]	[0.0001]	[0.0045]	[0.0206]
Block-reweighted	-0.027	-0.0092	-1.985	-0.279
	(0.014)	(0.0048)	(0.823)	(0.161)
	[0.0474]	[0.0534]	[0.0159]	[0.0837]
Drop rivers and rails	-0.033	-0.0163	-2.025	-0.339
	(0.011)	(0.0051)	(0.867)	(0.116)
	[0.0038]	[0.0014]	[0.0194]	[0.0034]
Drop and reweighted	-0.027	-0.0121	-1.7	-0.366
	(0.014)	(0.0056)	(0.994)	(0.145)
	[0.0465]	[0.0312]	[0.0871]	[0.0114]
Low-side μ	0.21	0.1229	7.547	1.698
Complier μ	0.157	0.097	5.114	1.308

*N*otes: This table reports RD estimates of the impact of HOLC grade increases using our baseline blocks × borders sample. Each column corresponds to a different gun violence measure and each row corresponds to a different specification. All regressions include city and border type fixed effects. The first four rows report results from linear RD specifications. In the second row, we reweight blocks the inverse of a block's number of observations in the blocks × border sample. In the third row, we drop borders which coincide with rivers and railroad tracks, as in Aaronson et al. (2021). In the fourth row, we both drop river and railroad borders and downweight blocks. Rows 5−8 report results from identical specifications estimated via the local polynomial approach from Calonico et al. (2014). For linear specifications, we report standard errors which are twoway clustered at the border and block level. For local polynomial specifications, we report standard errors clustered at the city-level, as well as robust p-values in brackets.

Figure 3: Grade-specific border discontinuity estimates

(a) Percent Minority

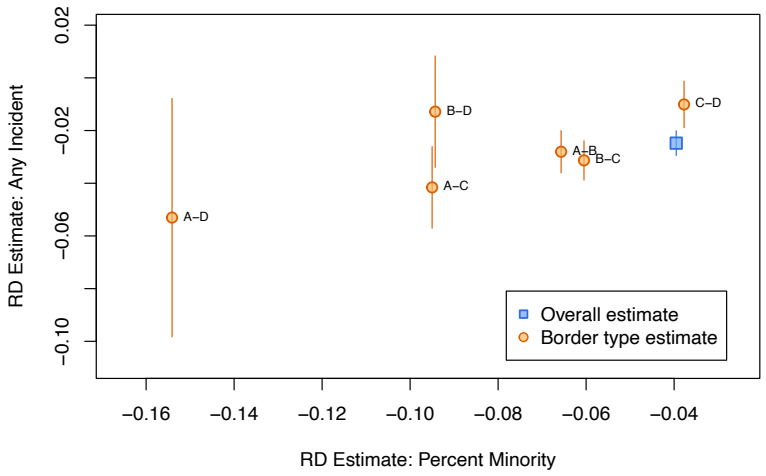

(b) Median household income

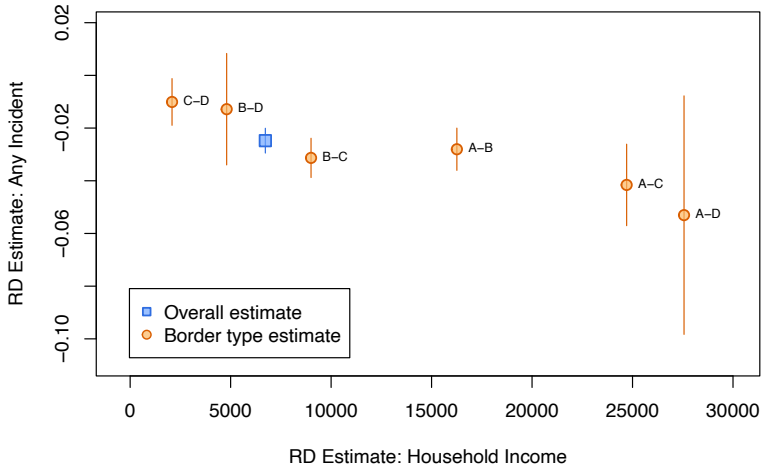

*N*otes: This figure reports RD estimates of the impact of HOLC grade increases for specific grade combinations. To construct panel (a), we estimate linear RD estimates of the impact of the "high" side on (i) any gun violence incident and (ii) percent minority, separately for each grade combination and conditional on city fixed effects. We then plot the RD estimate for gun violence (vertical axis) against the RD estimate for percent minority (horizontal axis), along with 95 confidence intervals. Panel (b) is constructed in an identical way except that RD estimates for median household income (measured at census block group-level) are reported on the horizontal axis.

Table 2: Decompositions of group disparities in exposure to neighborhood violence

	Minority (g) − White (h)		Poor (g) − Non-poor (h)	
	(1) Estimate	(2) Share	(3) Estimate	(4) Share
Between-city sorting ($\Delta^{c}_{g,h}$)	0.263	0.07	0.426	0.167
	(0.374)	(0.111)	(0.174)	(0.074)
Within-city × grade sorting ($\Delta^{q}_{g,h}$)	2.845	0.759	1.583	0.62
	(0.565)	(0.064)	(0.349)	(0.063)
Within-city outcome effect ($\Delta^{\tilde{v}}_{g,h}$)	0.093	0.025	0.127	0.05
	(0.175)	(0.053)	(0.17)	(0.069)
Within-city reweighting effet ($\Delta^{\tilde{\omega}}_{g,h}$)	0.261	0.07	0.285	0.112
	(0.066)	(0.028)	(0.061)	(0.028)
Within-city causal disparity ($\tilde{\Delta}_{g,h}$)	0.285	0.076	0.131	0.051
	(0.08)	(0.033)	(0.037)	(0.018)
Overall $\Delta_{g,h}$	3.747		2.553	
	(0.803)		(0.389)	
Benchmark $\bar{v}_h$	1.612		2.755	

*N*otes: This table reports estimates of the components of the group-level exposure disparity decomposition as described in section 5 and appendix D. Columns (1) and (2) report a decomposition of the Minority (Black and Hispanic) versus white exposure disparity while columns (3) and (4) report a decomposition of the below versus above poverty line exposure disparity. Columns (1) and (3) report estimated magnitudes of the associated component while columns (2) and (4) report the corresponding share of the overall disparity. Table footer reports the overall exposure disparity, as well as the benchmark average exposure for the reference group (h). Bootstrapped standard errors, clustered at the city-level, are reported in parentheses. Table B-9 reports decomposition estimates for alternative group definitions.

Appendix: For online publication

A Descriptive statistics

Figure A-1: Spatial concentration of crime across census tracts

(a) Land area

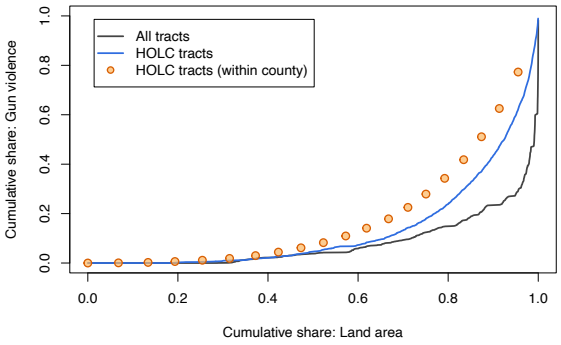

(b) Population

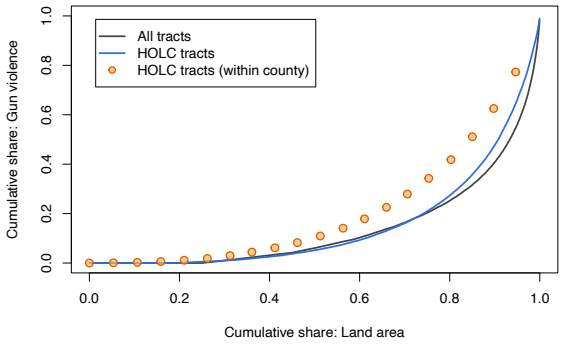

*N*otes: This figure depicts the spatial concentration of gun violence among all census tracts in the U.S. (solid gray line; $N = 73,057$) and among HOLC census tracts (solid blue line; $N = 15,018$). The figure is constructed by ranking census tracts from most to least violent (based on total incidents) and plotting the relationship between quantiles of violence and land area (left panel) and between quantiles of violence and population (right panel). For HOLC tracts, each panel also depicts a within-county version (orange circles), obtained by constructing 20 quantiles within each quantity and then aggregating up the count-specific estimates, weighting by county population shares.

Table A-1: Group differences in exposure to neighborhood gun violence

	(1) All	(2) All	(3) HOLC	(4) HOLC
By racial groups				
Black	3.635	2.546	6.715	5.571
	(0.468)	(0.392)	(1.107)	(1.096)
Hispanic	0.659	0.759	0.897	1.863
	(0.102)	(0.068)	(0.378)	(0.214)
Other race	0.252	0.298	0.262	1.274
	(0.058)	(0.045)	(0.246)	(0.126)
White μ	0.7004	0.7004	1.6122	1.6122
County FE	No	Yes	No	Yes
Tracts	73057	73057	15018	15018
By income groups (thousands)				
0–25	1.023	0.812	2.165	1.715
	(0.107)	(0.085)	(0.282)	(0.286)
25–50	0.471	0.390	1.111	0.852
	(0.044)	(0.038)	(0.144)	(0.149)
50–100	0.245	0.193	0.607	0.429
	(0.023)	(0.019)	(0.082)	(0.079)
100+ μ	1.1584	1.1584	2.8688	2.8688
County FE	No	Yes	No	Yes
Tracts	73057	73057	15018	15018

*N*otes: This table reports the regression estimates corresponding to figure 1. To obtain these regression estimates, we construct a stacked dataset which copies the set of census tracts once for each group g. In the stack for group g, we construct weights ω equal to share of group g residing in a given tract, as described in section 2. We then regress tract-level violence on the group "stack" indicators, clustering at the county-level and weighting by ω. This approach yields a coefficient on the group indicator exactly equal to $\Delta_{g,h} = \bar{v}_g - \bar{v}_h$ (using the notation of section 2), where h denotes the omitted group. The omitted category is white in the upper panel and household income $\geq$ \$100,00 in the lower panel. Note that the two panels correspond to separate regressions.

Table A-2: Group differences in exposure to neighborhood gun violence

	(1) All	(2) All	(3) HOLC	(4) HOLC
By race × poverty status				
White, poor	0.544	0.529	1.343	1.221
	(0.036)	(0.040)	(0.171)	(0.186)
Black, non-poor	3.156	1.935	5.879	4.621
	(0.426)	(0.337)	(1.057)	(1.040)
Black, poor	5.247	3.627	8.610	6.654
	(0.636)	(0.550)	(1.234)	(1.352)
Other, non-poor	0.330	0.312	0.381	1.231
	(0.070)	(0.096)	(0.252)	(0.177)
Other, poor	1.130	0.934	1.600	2.145
	(0.158)	(0.088)	(0.473)	(0.316)
White, non-poor μ	0.7052	0.7052	1.532	1.532
County FE	No	Yes	No	Yes
Tracts	73044	73044	15018	15018
By Hispanic status × poverty status				
Non-Hispanic, poor	1.543	1.173	3.440	2.553
	(0.181)	(0.162)	(0.458)	(0.513)
Hispanic, non-poor	0.146	0.309	-0.747	0.324
	(0.067)	(0.105)	(0.238)	(0.434)
Hispanic, poor	0.746	0.824	0.263	1.157
	(0.122)	(0.100)	(0.396)	(0.379)
Non-Hispanic, non-poor μ	1.0616	1.0616	2.9215	2.9215
County FE	No	Yes	No	Yes
Tracts	73044	73044	15018	15018

*N*otes: Same as table A-1 except that groups are defined as combination of race (upper panel) or ethnicity (lower panel) and poverty status (above or below the poverty line). As in table A-1, the two panels correspond to separate regressions because the ACS does not report counts at the race × ethnicity × poverty level. Also due to this constraint, the racial group definitions are slightly different in this table than in figure 1 and table A-1. In those exhibits, white Black, and other are defined as non-Hispanic, whereas in the upper panel of this table, these groups are inclusive of Hispanics.

Figure A-2: Census tract characteristics by HOLC grade

(a) Gun violence

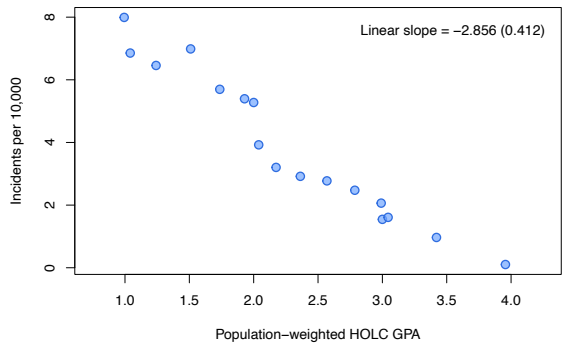

(b) Percent minority

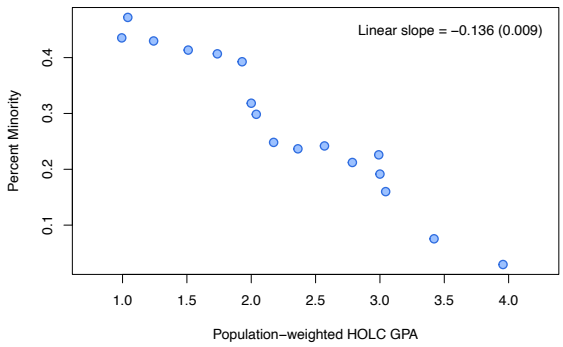

(c) Poverty rate

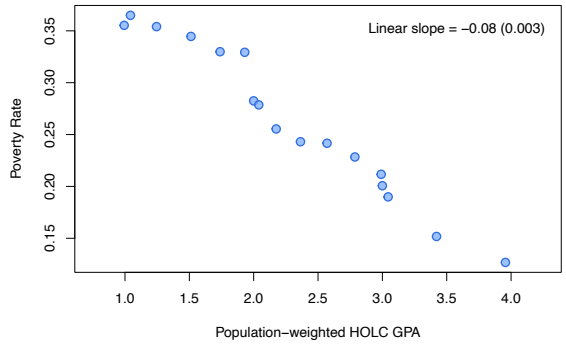

(d) Median household income

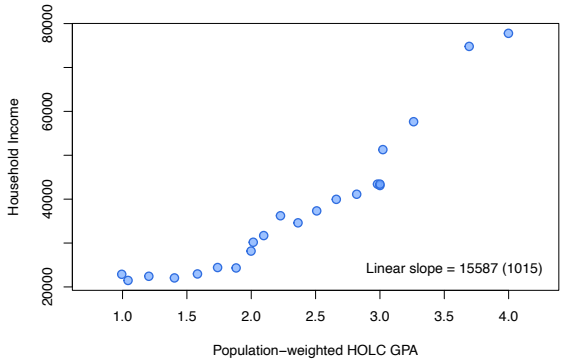

*N*otes: Each panel depicts a binned scatter of the relationship between a census tract characteristic and a tract's HOLC grade ("GPA"), adjusted for city fixed effects. The sample is tracts assigned to HOLC mapped areas ($N = 15,018$). Tract-level HOLC GPA is computed by taking the weighted average of grades for census blocks lying within a census tract, weighting by the share of the tract's population in each block. Blocks are graded by geocoding block centroids to HOLC polygons. Each panel reports the corresponding linear slope estimate and standard error clustered at the city-level.

Table A-3: Racial differences in exposure to neighborhood gun violence, block-level

	(1) All	(2) All	(3) All	(4) HOLC	(5) HOLC	(6) HOLC
By racial groups						
Black	3.395	2.518	0.312	6.625	5.681	0.442
	(0.397)	(0.331)	(0.017)	(1.092)	(1.071)	(0.061)
Hispanic	0.604	0.753	0.077	0.943	1.902	0.165
	(0.087)	(0.060)	(0.008)	(0.350)	(0.236)	(0.038)
Other race	0.254	0.336	0.087	0.336	1.375	0.197
	(0.050)	(0.041)	(0.007)	(0.234)	(0.143)	(0.035)
White μ	0.5481	0.5481	0.5481	1.3135	1.3135	1.3135
County FE	No	Yes	No	No	Yes	No
Tract FE	No	No	Yes	No	No	Yes
Blocks	6207027	6207027	6207027	541687	541687	541687

*N*otes: Same as table A-1 except at the census block, rather than census tract level. In this table, we add a specification which conditions on census tract fixed effects (columns 3 and 6).

Table A-4: Summary statistics, census blocks samples

	(1) All	(2) Graded	(3) Donut RD
Population	50	77	76
Land area (KM^2)	0.832	0.021	0.021
Percent minority	0.195	0.425	0.422
Percent poverty	0.156	0.228	0.23
Median household income	54811	51534	51451
Any incident	0.033	0.123	0.125
Incidents per 10,000	2.105	8	7.912
Blocks	6207027	540751	402024

*N*otes: This table reports summary statistics for various census blocks samples. Column 1 reports means for all census blocks (with positive population and land area) in the U.S. The second column reports means for the subset of census blocks that can be assigned HOLC grades, and the third column reports means for the subset of graded census blocks included in our donut RD sample. Population, race shares, and gun violence are measured directly at the census block-level. Poverty rates and household income are measured at the census block group-level and assigned to each census block included in that census block group.

Figure A-3: Geographic coverage of HOLC sample

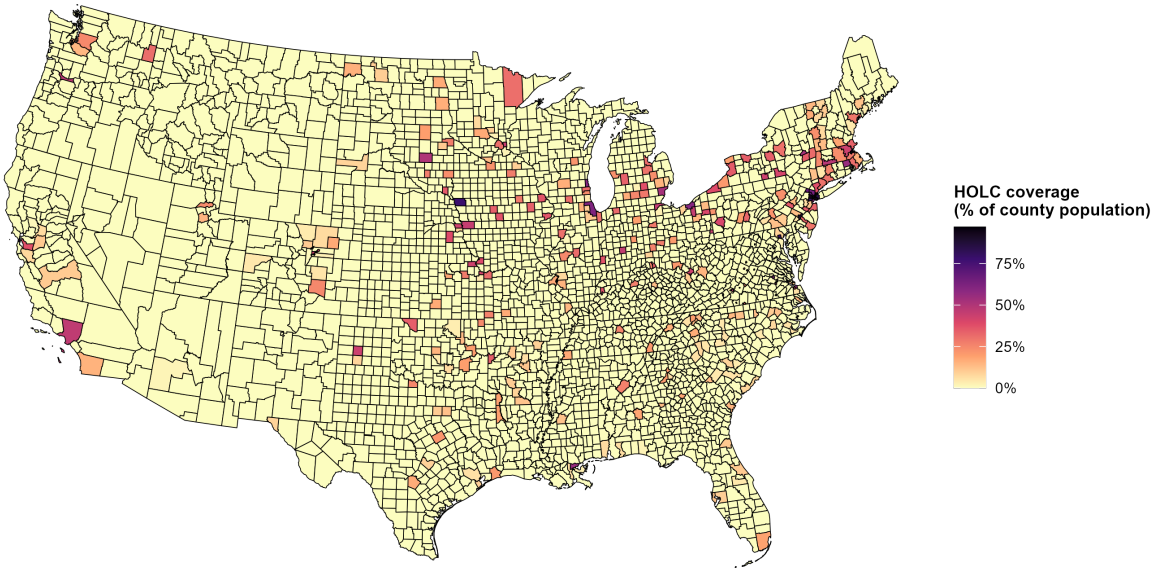

*N*otes: This figure reports the share of each county in the U.S. which is covered by our HOLC sample of census blocks.

B Border discontinuity analyses

Figure B-1: Distribution of incident-level distance from HOLC borders

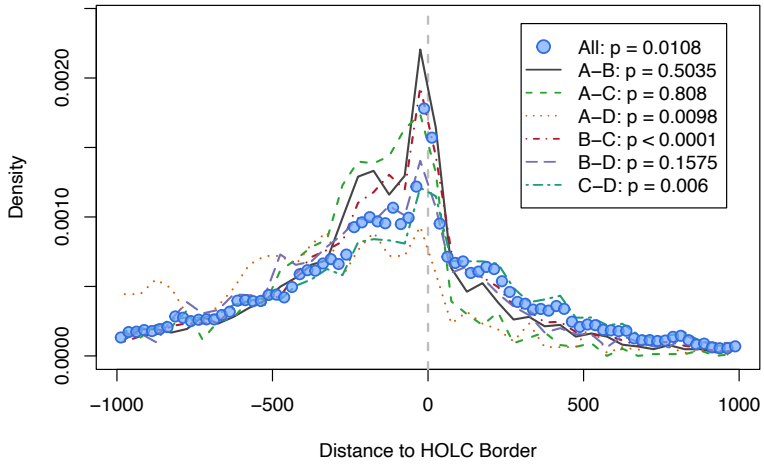

*N*otes: This figure depicts the distribution of gun violence incidents' distance (in meters) from HOLC polygon borders. Specifically, for each gun violence incident lying within HOLC areas, we geocode incidents to the nearest HOLC polygon border associated with a grade change and compute the distance to that border, with negative distances indicating the lower graded side of the border and positive distances indicating the higher graded side of the border. We then plot the distribution of distances, pooling all border types (i.e., grade combinations) together (blue circles) and for each grade combination (various line patterns and colors). The figure reports the p-values from the McCrary (2008) test for discontinuity in density at the border.

Figure B-2: Motivation for donut RD approach

(a) Share in HOLC polygon

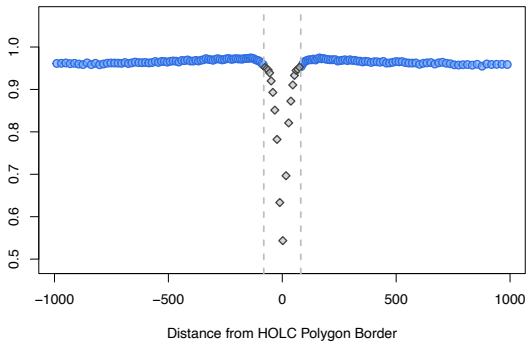

(b) Area-weighted GPA

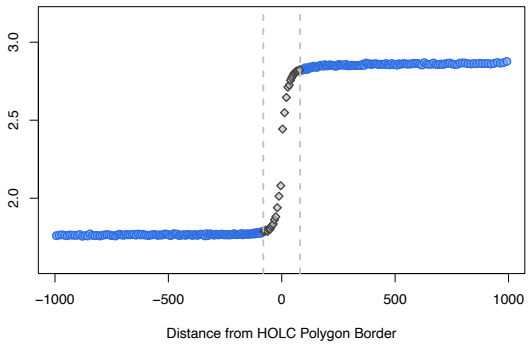

(c) Population

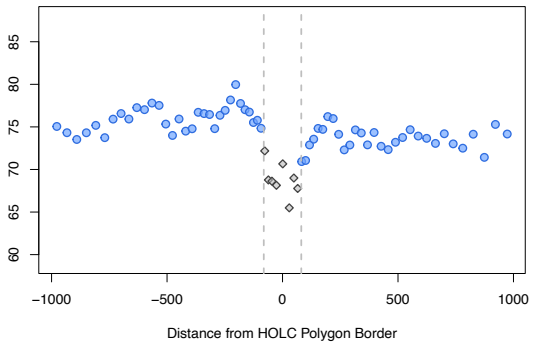

(d) Land area

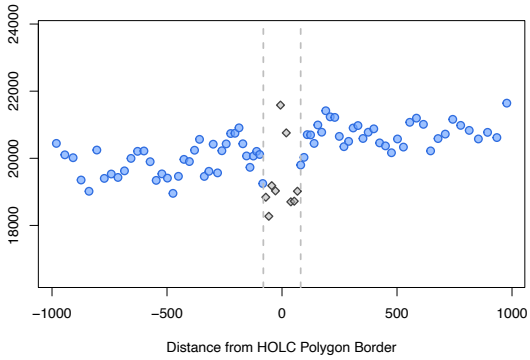

*N*otes: Each panel depicts a binscatter plot of the relationship between a census block's distance from a HOLC polygon border, where positive distance represents the higher graded side of the border (horizontal axis) and the denoted outcome (vertical axis). In panel (a), the outcome is the share of a census block's area lying within its designated HOLC polygon. In panel (b), the outcome is census block's area-weighted HOLC GPA, constructed by taking the average GPA of HOLC polygons overlapping the census block, weighting by area shares. In panels (c) and (d), the outcomes are a census blocks's population and land area (in square meters). Dashed vertical lines denote the "donut" used in our baseline sample (81.2 meters) and averages for blocks that lie within this donut are shown using gray diamonds. The sample in these plots is identical that used in our main analyses (e.g., figure 2) except that block × borders within the donut are included.

Figure B-3: Donut RD estimates for violence measures

(a) Any Incident

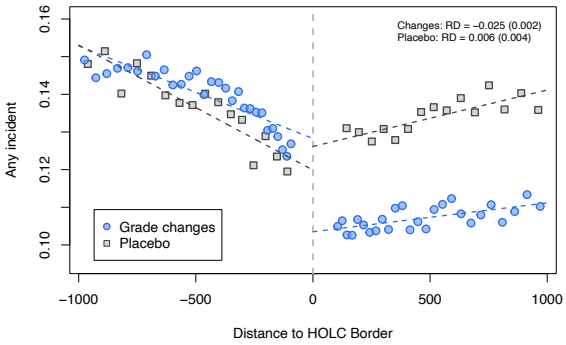

(b) Incidents

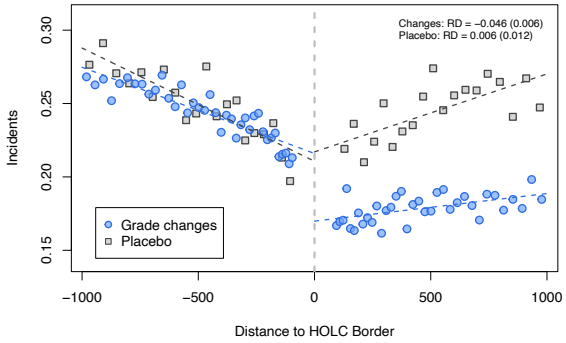

(c) Incidents per 10,000

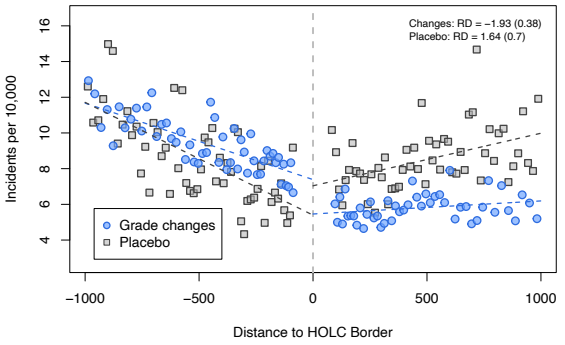

(d) Incidents per KM^2

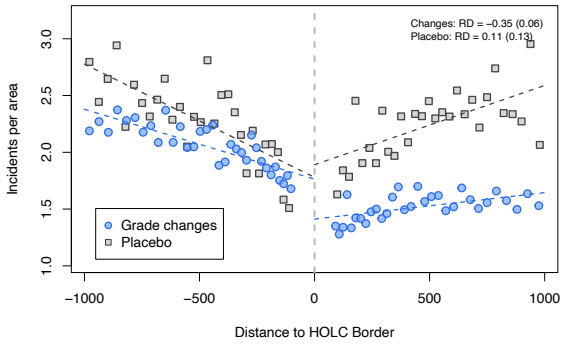

*N*otes: Same as figure 2 except for additional violence outcomes.

Figure B-4: Donut RD estimates for neighborhood characteristics

(a) Percent Minority

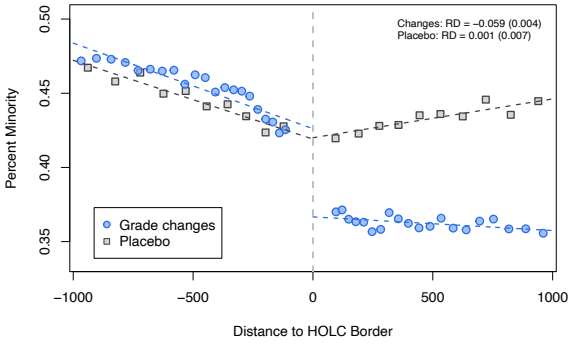

(b) Poverty rate

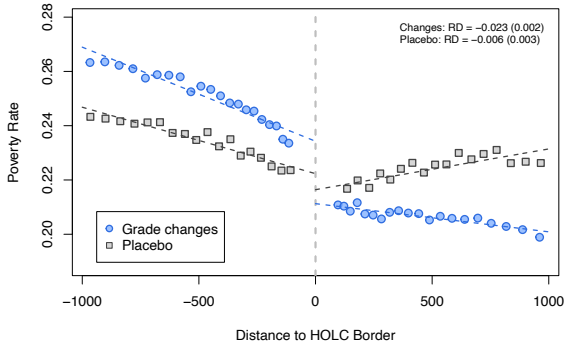

(c) Median household income

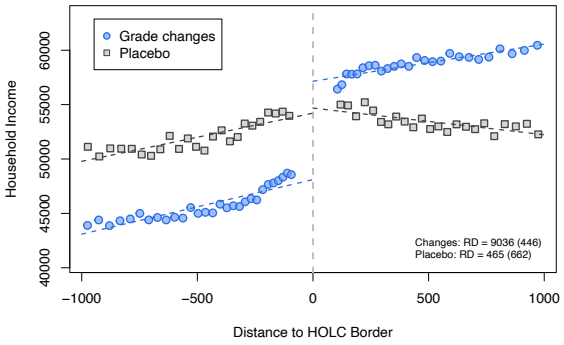

(d) Median home value

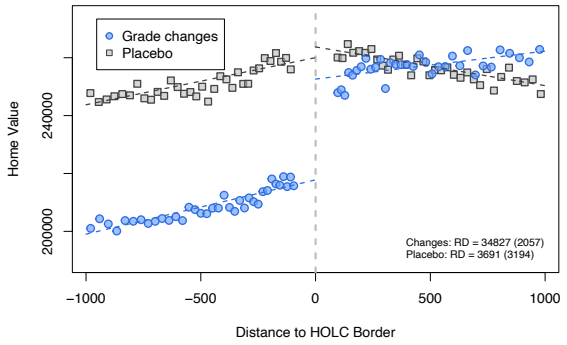

*N*otes: Same as figure 2 except for neighborhood characteristics.

Table B-1: Comparison between donut RD and OLS estimates

	(1) Incidents	(2) Any incident	(3) Incidents per 10,000	(4) Incidents per KM^2
OLS estimates (relative to A)				
Grade = B	0.086	0.0524	2.613	0.649
	(0.013)	(0.0063)	(0.468)	(0.143)
Grade = C	0.196	0.1063	6.962	1.644
	(0.028)	(0.0104)	(0.934)	(0.342)
Grade = D	0.274	0.1389	12.395	2.49
	(0.032)	(0.0118)	(1.352)	(0.459)
Implied effect of grade increase (comparable to RD)				
OLS estimate	-0.104	-0.0508	-4.903	-0.971
	(0.009)	(0.0033)	(0.373)	(0.111)
Baseline RD estimates				
Linear	-0.046	-0.0248	-1.927	-0.351
	(0.006)	(0.0024)	(0.382)	(0.064)
Local polynomial	-0.038	-0.0158	-2.134	-0.327
	(0.011)	(0.004)	(0.751)	(0.141)
μ (A graded)	0.05	0.0378	1.677	0.338

*N*otes: In the first panel, we report results from a regression of the denoted outcome on indicators for HOLC grades and city fixed effects estimated at the block-level using the sample of blocks included in our donut RD sample ($N = 402,024$). In the second panel, we report an estimate of the impact of a grade increase implied by the OLS estimates and meant to be comparable to our baseline RD estimate. Specifically, we compute the implied impact of moving across each border type by taking the all the pairwise comparisons implied by the OLS estimates and then compute a weighted average thereof, weighting by each grade combination's representation in our blocks $\times$ borders donut RD sample. In the third panel, we report our baseline RD estimates (same as those reported in table 1).

Table B-2: Comparison between donut RD and OLS estimates (neighborhood characteristics)

	(1) Percent Minority	(2) Poverty Rate	(3) Houseold Income	(4) Home Value
OLS estimates (relative to A)				
Grade = B	0.146	0.068	-30254	-114880
	(0.012)	(0.004)	(2165)	(9706)
Grade = C	0.276	0.141	-47807	-182987
	(0.02)	(0.005)	(2980)	(15859)
Grade = D	0.395	0.198	-54142	-205535
	(0.023)	(0.007)	(3045)	(16757)
Implied effect of grade increase (comparable to RD)				
OLS estimate	-0.143	-0.073	17541	66719
	(0.006)	(0.002)	(640)	(3801)
Baseline RD estimates				
Linear	-0.04	-0.013	6728	26163
	(0.005)	(0.002)	(473)	(2176)
Local polynomial	-0.035	-0.015	5607	23811
	(0.005)	(0.002)	(436)	(1948)
μ (A graded)	0.19	0.12	89883	366062

*N*otes: Same as table B-1 except for neighborhood characteristics.

Table B-3: Donut RD estimates, varying fixed effects

	(1) Incidents	(2) Any incident	(3) Incidents per 10,000	(4) Incidents per KM^2
Linear estimates				
None	-0.039	-0.0201	-1.371	-0.296
	(0.006)	(0.0027)	(0.391)	(0.072)
City	-0.031	-0.0174	-1.276	-0.207
	(0.006)	(0.0024)	(0.384)	(0.064)
Border type	-0.052	-0.0265	-1.965	-0.424
	(0.006)	(0.0027)	(0.39)	(0.073)
City and Border type	-0.046	-0.0248	-1.927	-0.351
	(0.006)	(0.0024)	(0.382)	(0.064)
City × Border type	-0.045	-0.024	-1.851	-0.343
	(0.006)	(0.0023)	(0.387)	(0.064)
Border	-0.045	-0.0229	-2.045	-0.323
	(0.005)	(0.0021)	(0.39)	(0.053)
Local polynomial estimates				
None	-0.037	-0.0137	-2.03	-0.368
	(0.022)	(0.0092)	(0.997)	(0.25)
	[0.082]	[0.1366]	[0.0417]	[0.1408]
City	-0.031	-0.0124	-1.857	-0.265
	(0.012)	(0.0042)	(0.759)	(0.142)
	[0.0075]	[0.0028]	[0.0144]	[0.0608]
Border type	-0.043	-0.0166	-2.275	-0.423
	(0.022)	(0.0094)	(1.006)	(0.25)
	[0.049]	[0.0772]	[0.0237]	[0.0911]
City and Border type	-0.038	-0.0158	-2.134	-0.327
	(0.011)	(0.004)	(0.751)	(0.141)
	[0.0008]	[0.0001]	[0.0045]	[0.0206]
City × Border type	-0.037	-0.0149	-2.113	-0.327
	(0.011)	(0.0039)	(0.734)	(0.131)
	[0.0007]	[0.0001]	[0.004]	[0.0125]
Low-side μ	0.21	0.1229	7.547	1.698
Complier μ	0.157	0.097	5.114	1.308

*N*otes: Same as table 1 except that each different specification corresponds to a different set of conditioning fixed effects. The third row in each panel corresponds to our baseline specification which includes city and border type (i.e., grade combination) fixed effects.

Table B-4: Donut RD estimates, other violence outcomes

	(1) Low-side μ	(2) Linear	(3) Local polynomial
Baseline, winsorized			
Incidents	0.207	-0.03	-0.037
		(0.006)	(0.011)
Incidents per 10,000	7.046	-1.426	-1.928
		(0.28)	(0.497)
Incidents per KM^2	1.656	-0.21	-0.296
		(0.058)	(0.123)
Victims with injury or fatality			
Injuries	0.262	-0.041	-0.05
		(0.008)	(0.015)
Any Injury	0.123	-0.017	-0.016
		(0.002)	(0.004)
Injuries per 10,000	9.342	-1.583	-2.414
		(0.533)	(1.08)
Injuries per KM^2	2.112	-0.291	-0.426
		(0.084)	(0.185)
Victims with fatality			
Deaths	0.071	-0.01	-0.013
		(0.002)	(0.003)
Any Death	0.053	-0.007	-0.007
		(0.001)	(0.002)
Deaths per 10,000	2.567	-0.443	-0.741
		(0.171)	(0.288)
Deaths per KM^2	0.561	-0.065	-0.091
		(0.023)	(0.036)

*N*otes: This table reports donut RD estimates at grade change borders using our baseline block $\times$ border sample for various outcome measures. The first panel reports estimates when winsorizing our baseline outcome measures at the 99.9th percentile. The second panel reports estimates replacing the number of incidents with the number of victims with an injury or fatality. The third panel reports estimates replacing the number of incidents with the number of fatalities. Column (1) reports the complier mean for the relevant outcome. Column (2) reports the linear RD estimate and column (3) reports the bias-corrected local polynomial estimate from Calonico et al. (2014). All estimates condition on city and border type (i.e., grade combination) fixed effects. For linear estimates, we report standard errors which are twoway clustered at the block and border level. For local polynomial estimates, we report standard errors clustered at the city level.

Table B-5: Donut RD estimates, neighborhood outcomes

	(1) Low-side μ	(2) Linear	(3) Local polynomial
Neighborhood outcomes			
Percent Black	0.248	-0.021	-0.019
		(0.004)	(0.005)
Percent Minority	0.413	-0.04	-0.035
		(0.005)	(0.005)
Poverty rate	0.23	-0.013	-0.015
		(0.002)	(0.002)
Median household income	49719	6728	5607
		(473)	(436)
Median home value	225432	26163	23811
		(2176)	(1948)
Median rent	943	28	30
		(4)	(4)

*N*otes: This table reports donut RD estimates at grade change borders using our baseline block × border sample for various outcome measures. Column (1) reports the complier mean for the relevant outcome. Column (2) reports the linear RD estimate and column (3) reports the bias-corrected local polynomial estimate from Calonico et al. (2014). All estimates condition on city and border type (i.e., grade combination) fixed effects. For linear estimates, we report standard errors which are twoway clustered at the block and border level. For local polynomial estimates, we report standard errors clustered at the city level. Note that only racial composition is directly measured at the census-block level; other outcomes are measured at the census block group level and then assigned to all blocks within that block group.

Figure B-5: RD estimates varying donut and bandwidth size

(a) Varying donut: Any incident

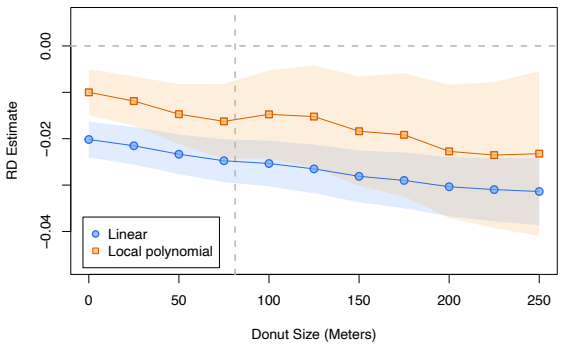

(b) Varying donut: Incidents

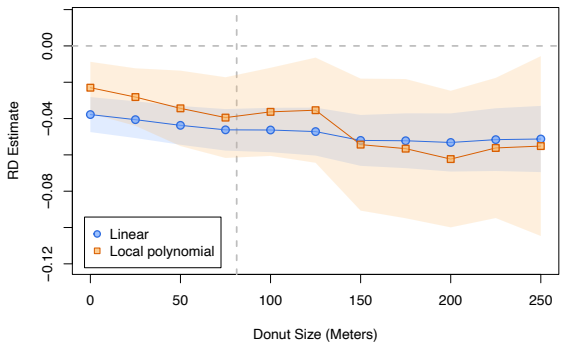

(c) Varying bandwidth: Any incident

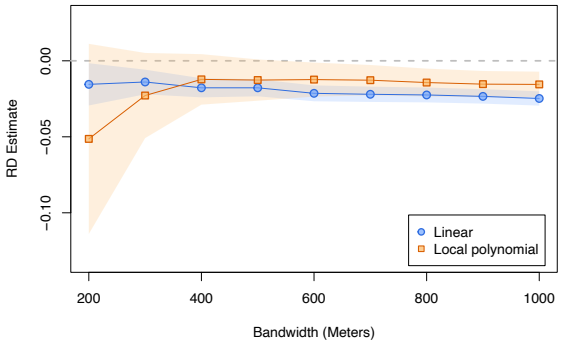

(d) Varying bandwidth: Incidents

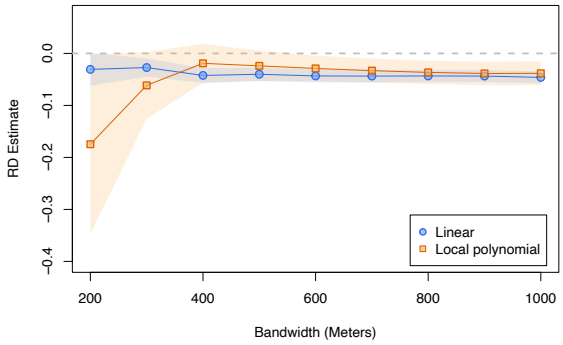

Notes: This figure reports linear and bias-corrected local polynomial (Calonico et al., 2014) donut RD estimates, with associated 95 percent confidence bands, for gun violence outcomes when varying the size of the "donut" and when varying the choice of bandwidth. In panels (a) and (b), we hold the bandwidth fixed at 1000 meters and vary the size of the "donut" – i.e., in these two panels, the estimate at a given value of the horizontal axis x is the estimate when dropping census blocks whose centroids are within x meters of the border. The dashed vertical decline denotes our baseline donut choice (= 81.2 meters) In panel (c) and (d), we hold the size of the donut fixed at our baseline donut and vary the size of the bandwidth – i.e., in these two panels, the estimate at a given alue of the horizontal axis x is the estimate when keep census blocks whose centroids are between 81.2 meters and x meters are the border.

Table B-6: Distribution of border types (grade combinations) and associated characteristics

	Borders		Blocks × Borders		Complier μ			
	(1)	(2)	(3)	(4)	(5)	(6)	(7)	(8)
	N	Share	N	Share	Any Incident	Percent Minority	Percent Povery	Household Income
D–A	102	0.012	7113	0.01	0.044	0.269	0.156	84864
D–B	2757	0.313	250789	0.348	0.152	0.508	0.281	40272
D–C	460	0.052	34000	0.047	0.086	0.371	0.236	48657
C–A	500	0.057	30192	0.042	0.04	0.208	0.139	80637
C–B	3398	0.386	287309	0.399	0.09	0.323	0.19	58284
B–A	1584	0.18	111437	0.155	0.034	0.178	0.118	87475

*N*otes: This table reports donut RD estimates at grade change borders using our baseline block × border sample for various outcome measures. The first panel reports estimates when winsorizing our baseline outcome measures at the 99.9th percentile. The second panel reports estimates replacing the number of incidents with the number of victims with an injury or fatality. The third panel reports estimates replacing the number of incidents with the number of fatalities. Column (1) reports the complier mean for the relevant outcome. Column (2) reports the linear RD estimate and column (3) reports the bias-corrected local polynomial estimate from Calonico et al. (2014). All estimates condition on city and border type (i.e., grade combination) fixed effects. For linear estimates, we report standard errors which are twoway clustered at the block and border level. For local polynomial estimates, we report standard errors clustered at the city level.

Table B-7: Donut RD estimates by border type (grade combination)

	(1) Incidents	(2) Any incident	(3) Incidents per 10,000	(4) Incidents per KM^2
Linear estimates				
D–A	-0.099	-0.053	-0.66	-0.584
	(0.041)	(0.0231)	(3.909)	(0.306)
D–B	-0.028	-0.0101	-1.618	-0.182
	(0.012)	(0.0045)	(0.941)	(0.147)
D–C	-0.015	-0.0128	-3.108	0.228
	(0.031)	(0.0108)	(1.71)	(0.359)
C–A	-0.06	-0.0416	-2.237	-0.306
	(0.017)	(0.0079)	(0.805)	(0.146)
C–B	-0.058	-0.0313	-2.28	-0.493
	(0.009)	(0.0038)	(0.467)	(0.087)
B–A	-0.036	-0.028	-0.693	-0.319
	(0.007)	(0.0041)	(0.445)	(0.092)
Local polynomial estimates				
D–A	-0.103	0.0142	9.434	-0.207
	(0.126)	(0.0473)	(7.814)	(0.845)
D–B	-0.034	-0.0044	-2.031	-0.382
	(0.024)	(0.0085)	(1.724)	(0.291)
D–C	-0.021	-0.0191	2.196	-0.029
	(0.043)	(0.0223)	(3.572)	(0.342)
C–A	0.063	0.0563	1.753	0.203
	(0.043)	(0.0246)	(3.095)	(0.323)
C–B	-0.048	-0.0183	-2.705	-0.349
	(0.012)	(0.0055)	(0.846)	(0.119)
B–A	-0.016	-0.0219	-0.749	-0.04
	(0.012)	(0.0056)	(0.702)	(0.146)

*N*otes: This table reports donut RD estimates at grade change borders for subsamples of our baseline block × border sample based on a border's grade combination (i.e., the first row reports estimates for borders between D- and A-graded polygons). As in table 1, the upper panel reports estimates using a specification and the lower panel reports bias-corrected local polynomial estimates from Calonico et al. (2014).

Table B-8: Donut RD estimates by border type (grade combination)

	(1) Percent Black	(2) Percent Minority	(3) Percent Poverty	(4) Median Income	(5) Median Value	(6) Median Rent
Linear estimates						
D–A	-0.101	-0.154	-0.055	27563	132090	88
	(0.038)	(0.041)	(0.034)	(5971)	(36009)	(58)
D–B	-0.024	-0.038	-0.012	2084	10368	27
	(0.008)	(0.008)	(0.004)	(760)	(3624)	(7)
D–C	-0.056	-0.094	-0.019	4803	32153	20
	(0.014)	(0.016)	(0.008)	(1500)	(5584)	(14)
C–A	-0.044	-0.095	-0.058	24707	97035	70
	(0.015)	(0.016)	(0.008)	(2571)	(10031)	(22)
C–B	-0.032	-0.06	-0.025	9002	32286	40
	(0.006)	(0.006)	(0.003)	(568)	(2752)	(5)
B–A	-0.039	-0.066	-0.027	16259	56417	42
	(0.007)	(0.008)	(0.004)	(1262)	(5385)	(10)
Local polynomial estimates						
D–A	-0.035	-0.023	-0.014	-12104	142763	-32
	(0.044)	(0.077)	(0.039)	(42258)	(118042)	(84)
D–B	-0.002	-0.009	-0.007	301	3473	8
	(0.009)	(0.009)	(0.004)	(664)	(3766)	(10)
D–C	-0.032	-0.031	-0.021	1209	-15225	-33
	(0.02)	(0.023)	(0.011)	(2064)	(12283)	(26)
C–A	0.066	0.004	-0.003	12314	52865	61
	(0.033)	(0.029)	(0.021)	(2835)	(10370)	(32)
C–B	-0.024	-0.044	-0.016	4385	21577	38
	(0.007)	(0.007)	(0.003)	(617)	(3085)	(5)
B–A	-0.015	-0.03	-0.012	10054	33638	6
	(0.009)	(0.011)	(0.005)	(1711)	(7354)	(10)

*N*otes: This table reports donut RD estimates at grade change borders for subsamples of our baseline block × border sample based on a border's grade combination (i.e., the first row reports estimates for borders between D- and A-graded polygons). As in table 1, the upper panel reports estimates using a specification and the lower panel reports bias-corrected local polynomial estimates from Calonico et al. (2014).

Figure B-6: Grade-specific RD estimates: Any incident, linear

(a) Percent minority

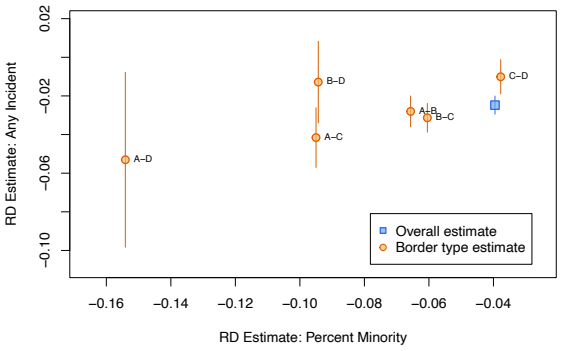

(b) Poverty rate

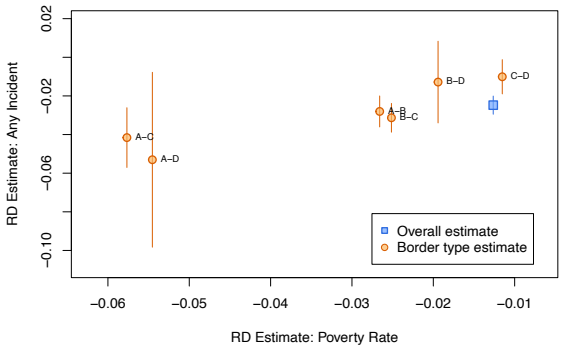

(c) Median household income

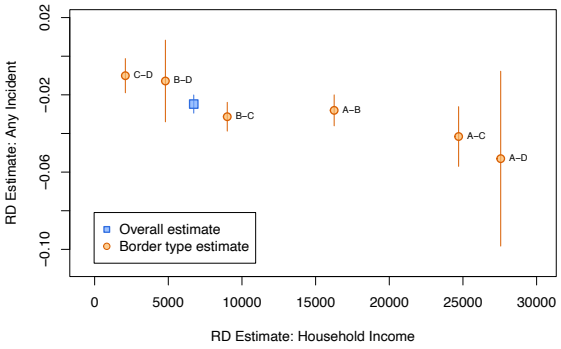

(d) Median home value

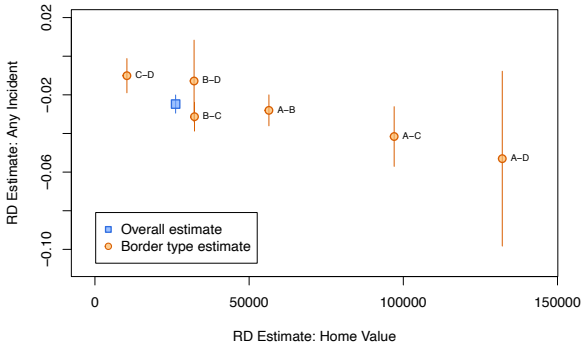

*N*otes: Same as figure 3, for additional neighborhood outcomes.

Figure B-7: Grade-specific RD estimates: Any incident, local polynomial

(a) Percent minority

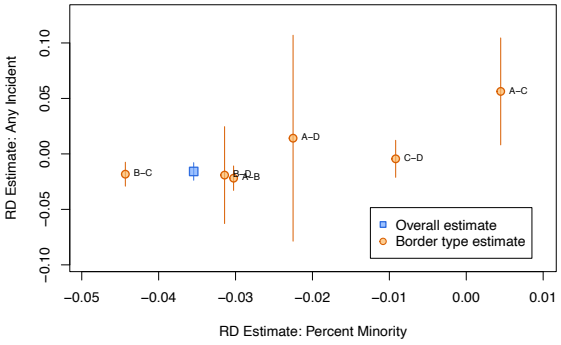

(b) Poverty rate

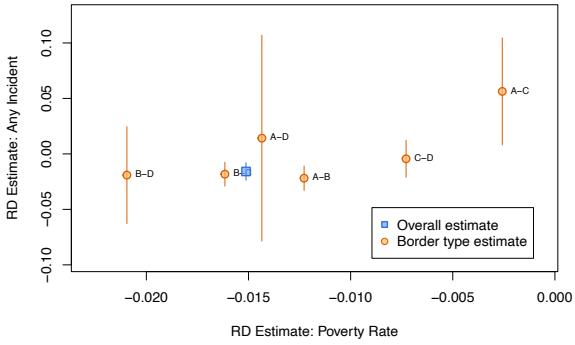

(c) Median household income

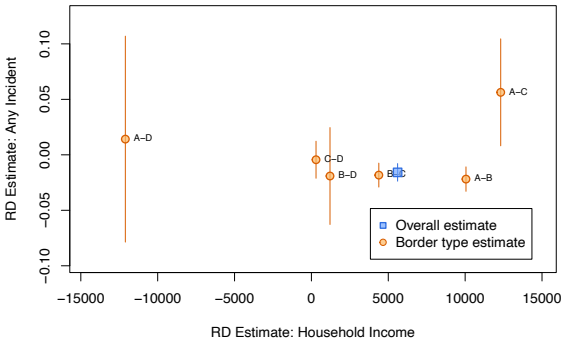

(d) Median home value

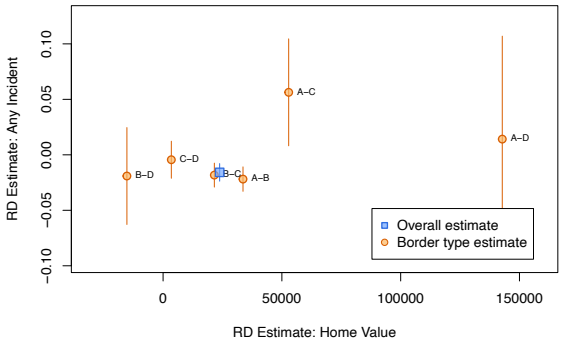

Notes: Same as figure B-6, using robust local polynomial estimates (Calonico et al., 2014) instead of linear estimates.

Table B-9: Exposure disparity decompositions (alternative groups)

	Black (g) − White (h)		\$0-25 (g) − \$100+ (h)	
	(1) Estimate	(2) Share	(3) Estimate	(4) Share
Between-city sorting ($\Delta^{c}_{g,h}$)	1.539	0.229	0.427	0.147
	(0.331)	(0.056)	(0.316)	(0.115)
Within-city × grade sorting ($\Delta^{q}_{g,h}$)	4.517	0.672	1.7	0.586
	(0.967)	(0.05)	(0.349)	(0.065)
Within-city outcome effect ($\Delta^{\tilde{v}}_{g,h}$)	0.142	0.021	0.293	0.101
	(0.272)	(0.043)	(0.335)	(0.118)
Within-city reweighting effet ($\Delta^{\tilde{\omega}}_{g,h}$)	0.249	0.037	0.217	0.075
	(0.071)	(0.011)	(0.046)	(0.017)
Within-city causal disparity ($\tilde{\Delta}_{g,h}$)	0.273	0.041	0.264	0.091
	(0.086)	(0.017)	(0.073)	(0.029)
Overall $\Delta_{g,h}$	6.719		2.9	
	(1.06)		(0.367)	
Benchmark $\bar{v}_h$	1.612		2.137	

*N*otes: Same as table 2 except for alternative group definitions.

C Results from Hynsjo & Perdoni (2024) approach

Hynsjo & Perdoni (2024) propose an alternative approach for evaluating the impact of HOLC grading based on comparisons between graded areas and observably similar areas which were not graded, because only cities with populations exceeding 40,000 were mapped, an institutional feature also used for identification in Anders (2023).

Their strategy is to divide cities into hexagons of about 7.3 acres per hexagon, roughly approximating the size of a city block. They then train a random forest model to predict HOLC grades for each hexagon based on information from the 1930 full count census and estimate difference-in-differences models which compare the change over time in outcomes for hexagons predicted to receive the same grade in areas which were and were not mapped. Their sample of interest is comprised of cities near the 40,000 population threshold as of 1930, specifically 97 cities with populations between 30,000 and 60,000.

We use this exact sample of cities and implement a modified version of their strategy.[11] Specifically, we geocode gun violence incidents into their hexagons and then compare violence in areas predicted receive each grade A−D in cities which were and were not mapped due to their falling above and below the population threshold for a HOLC survey.

These comparisons are depicted in figure C-1, which shows average present day outcomes for each predicted grade for areas with populations above 40,000 in 1930 and thus were mapped by the HOLC (blue circles, "treated") and for areas with populations below 40,000 in 1930 and thus were not mapped by HOLC (orange squares, "control"). These figures illustrate (i) that neighborhoods predicted to receive lower grades based on their 1930 characteristics exhibits higher levels of violence today and (ii) the differences across grades is more pronounced among cities that were mapped than those that were not. This steeper gradient for mapped cities suggests that HOLC designations matter for present day violence levels above and beyond an area's pre-HOLC characteristics.

One could think of this approach as yielding a difference-in-differences estimate for each pair of grades (g, h), with g the higher grade and h the lower grade in pair (g, h):

$$\theta_{g,h}^{DiD} = \Big(E(y|g, D = 1) - E(y|h, D = 1)\Big) - \Big(E(y|g, D = 0) - E(y|h, D = 0)\Big),$$

where D is an indicator for whether the city falls above the 40,000 population threshold for HOLC mapping. If $g = A$ and $h = D$, for example, the above DiD estimate quantifies the extent to which outcomes differ for hexagons predicted to receive grades of A and D in cities which were and were not actually mapped. This DiD estimate corresponds to the causal effect of HOLC mapping on the g, h difference under the assumption that g and h areas would have evolved similarly over time had there been no HOLC mapping.

To construct an overall estimate which corresponds closely to our baseline RDD estimate, we first compute $\theta_{g,h}^{DiD}$ for each combination of grades. We then average these grade combination-specific DiD estimates, weighting by each grade combination's representation in our boder discontinuity sample for comparability with our RDD estimates. These estimates

[11] See appendix A.5 in Hynsjo & Perdoni (2024) for the list of cities. We cannot copy their strategy exactly because we do not observe gun violence prior to HOLC mapping. Instead, we make comparisons between predicted grades for cities that were and were not mapped.

and associated standard errors (clustered at the city-level) are reported in each panel of figure C-1. For any gun violence incident, the weighted average estimate is -0.034 ($se = 0.0166$) and for incidents per KM^2, the weighted average estimate is -0.25 ($se = 0.106$). Both are statistically significant at the five percent level and both are comparable to the corresponding border discontinuity estimates reported in table 1.

Figure C-1: DiD estimates based on modified Hynsjo & Perdoni (2024) approach

(a) Any incident

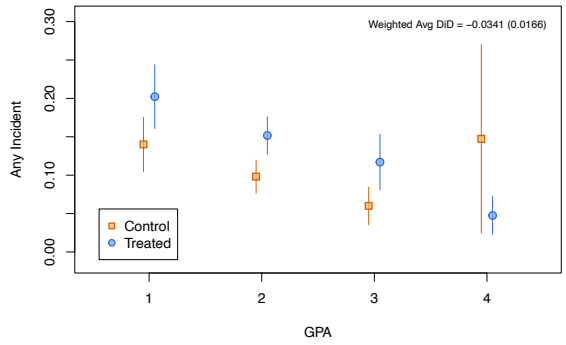

(b) Incidents per KM^2

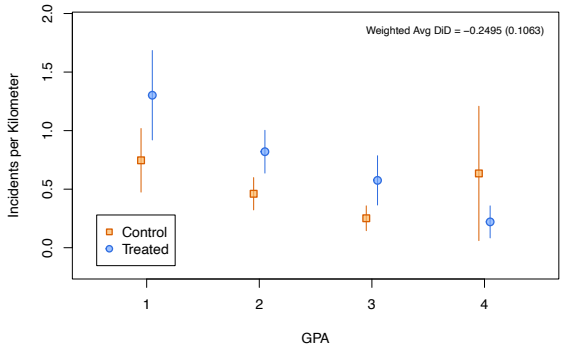

*N*otes: This figure reports estimates based on our modified version of the DiD approach from Hynsjo & Perdoni (2024). Orange squares report average outcomes for polygons predicted to receive a given grade (denoted as GPA on the horizontal axis) based on their pre-HOLC observables but were located in cities that were not actually mapped due to falling below the 40,000 population threshold. Blue circles report average outcomes for polygons predicted to receive a given grade and were actually mapped. For additional details, see Hynsjo & Perdoni (2024). In each figure, we report a weighted average of grade-specific DiD estimates as follows by computing the DiD estimate for each grade combination and taking a weighted average, weighting by each grade combination's representation in our border discontinuity sample.

D Decomposition exercise

In section 5, we compute a decomposition of group disparities in exposure to neighborhood (census tract) violence, using the exposure measure introduced in section 2. The full decomposition is written as:

$$\begin{aligned}
\Delta_{g,h} &\equiv \sum_j \omega_{gj} v_j - \sum_j \omega_{hj} v_j = \sum_j (\omega_{gj} - \omega_{hj}) v_j \\
&= \underbrace{\sum_c (\omega_{gc} - \omega_{hc}) v_c}_{\text{between-}c\text{ variation}} + \underbrace{\sum_j (\omega_{gj} - \omega_{hj})(v_j - v_{q(j)})}_{\text{within-}q\text{ variation}} \\
&\quad + \underbrace{\sum_q (\omega_{gq} - \omega_{hq}) \Big[(v_q - v_{c(q)}) - (\tilde{v}_q - v_{c(q)}) \Big]}_{\text{within-}c\text{ outome effect}} \\
&\quad + \underbrace{\sum_q \Big[(\omega_{gq} - \omega_{hq}) - (\tilde{\omega}_{gq} - \tilde{\omega}_{hq}) \Big] \big(\tilde{v}_q - v_{c(q)} \big)}_{\text{within-}c\text{ reweighting effect}} \\
&\quad + \underbrace{\sum_q (\tilde{\omega}_{gq} - \tilde{\omega}_{hq}) \big(\tilde{v}_q - v_{c(q)} \big)}_{\text{within-}c\text{ causal disparity}} .
\end{aligned}$$

where c denotes cities, q denotes cells at the level of city $\times$ HOLC grades. In this decomposition, $\tilde{v}_q$, $\tilde{\omega}_{gq}$, and $\tilde{\omega}_{hq}$ denote "causal counterfactuals" defined at the q-level. Here we provide a detailed description of how these quantities are calculated.

For ease of notation, replace q with (c, d) where c denotes city and d denotes HOLC grades. To construct the causal counterfactual level of gun violence $\tilde{v}_{c,d}$, we use the causal slope between violence v and HOLC grade implied by the border discontinuity estimates. Specifically, using our blocks (i) $\times$ borders (b) regression discontinuity sample, we estimate:

$$v_{ib} = \beta GPA_{ib} + f(\delta_{ib}) + X_i + \epsilon_{ib},$$

instrumenting GPA with an indicator for whether block i is on the higher graded side of border b. Following our baseline approach, we include city and border type fixed effects and parameterize distance from the border δ linearly. We then compute $\tilde{v}_{c,d}$ as:

$$\tilde{v}_{c,d} = \underbrace{E(v|c)}_{\text{average } v \text{ in city } c} - \Big(\beta \cdot \underbrace{E(d|c)}_{\text{average } d \text{ in city } c} \Big) + \beta d$$

In other words, $\tilde{v}_{c,d}$ holds constant the average v in city c but replaces the observed slope in the relationship between v and d with the causal slope implied by our baseline border discontinuity estimates.

We use the same idea to estimate the "causal counterfactual" weights $\tilde{\omega}_{gq}$ and $\tilde{\omega}_{hq}$, al-

though this requires an additional step worth clarifying. Specifically, let $p^g_{c,d}$ denote the share of residents in cell (c,d) who belong to group g. We construct causal counterfactuals for this quantity as above:

$$\tilde{p}^g_{c,d} = \underbrace{E(p^g|c)}_{\text{average } p \text{ in city } c} - \left(\beta \cdot \underbrace{E(d|c)}_{\text{average } d \text{ in city } c}\right) + \beta d$$

where now β is the causal slope from applying our border discontinuity estimates with p^g as the outcome of interest. Given $\tilde{p}^g_{c,d}$, Bayes rule implies the corresponding $\tilde{\omega}_{g,c,d}$:

$$\tilde{\omega}_{g,c,d} = Pr(c,d|g) = \frac{Pr(g|c,d)Pr(c,d)}{Pr(g)} = \frac{\tilde{p}^g_{c,d}Pr(c,d)}{Pr(g)}$$

where $Pr(c,d)$ and $Pr(g)$ are population shares in cell (c,d) and group g, respectively.

E Data appendix

E-1 Validation of GVA data

We conduct two exercises to validate the Gun Violence Archive (GVA) data. First, we compare fatalities reported in the GVA data with publicly reported data on firearm deaths from the CDC Wonder files (Multiple Cause of Death 2014–2017; Provisional Multiple Cause of Death 2018–present). At the state × year level, we compare the rate of firearm fatalities reported by CDC with the rate we compute from the GVA data.

Panel (a) of figure E-1 depicts the raw correlation between the two measures of gun violence, while panel (b) depicts the relationship conditional on state and year fixed effects. We find that gun fatalities reported in the GVA data closely track official CDC counts both overall and within-state, suggesting a high degree of coverage of firearm violence in the GVA daata, consistent with the validation exercise from Gobaudet al. (2023).

Our second validation exercise provides neighborhood-level comparisons between the prevalence of gun violence incidents from the GVA and the prevalence of crime more broadly, using geocoded incident-level data made available by a select set of police departments and aggregated by OpenPoliceData.[12] We accessed incident-level records compiled by OpenPoliceData (OPD) via their Python library. We identified 13 cities providing incident-level crime information with geographic coordinates.[13]

For these cities, we geocode incidents into census tracts and then explore the relationship between tract-level reported crimes from OPD and tract-level gun violence from GVA in panel (c) of figure E-1, which illustrates the relationship between a tract's incidents per 100,000 residents in the OPD data on the horizontal axis and a tract's gun violence per 100,000 residents from GVA on the vertical axis.

[12] See https://github.com/openpolicedata/openpolicedata.

[13] The cities are Los Angeles, CA; San Diego, CA; Santa Rosa, CA; Montgomery County, MD; Boston, MA; Cambridge, MA; Detroit, MI; Minneapolis, MN; Buffalo, NY; Cary, NC; Cincinnati, OH; and Mount Pleasant, SC.

Figure E-1: GVA validation exercises

(a) CDC

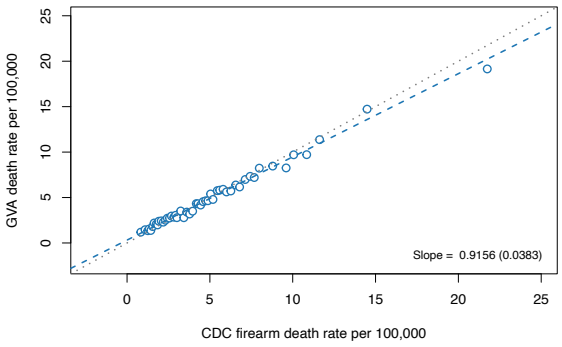

(b) CDC (residualized)

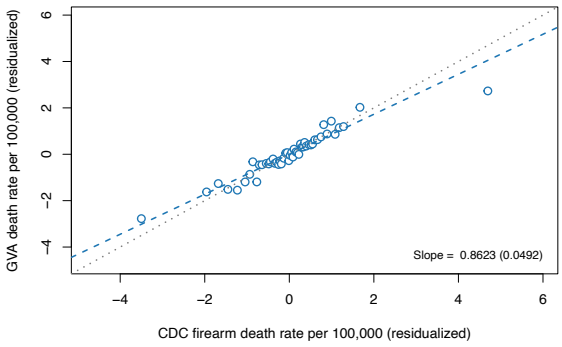

(c) OPD

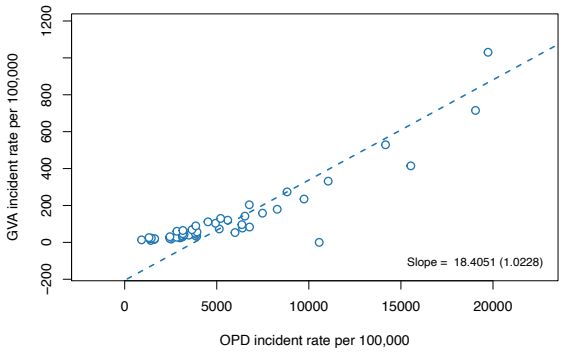

*N*otes: Panel (a) illustrates the relationship between firearm deaths reported in the CDC Wonder data (horizontal axis) and gun fatalities reported in the GVA data (vertical axis) per 100,000 residents at the state-year level. Panel (b) illustrates the same relationship, residualized of state and year fixed effects. Panel (c) illustrates the relationship between tract-level reported crime incidents per 100,000 residents and tract-level GVA incidents per 100,000 residents for 13 cities with geocoded incident data, as described above.

E-2 Construction of border segments

To construct the HOLC border dataset used in the analysis, we began with the digitized HOLC neighborhood polygons from the Mapping Inequality project (Nelson et al., 2021). We processed the data using various commands available in the `sf` package for R (Pebesma, 2018), first cleaning the HOLC polygons by repairing invalid geometries (`st_make_valid` as well as some buffer-based fixes), dropping empty geometries, standardizing grade values, and snapping coordinates to a fine grid (`lwgeom`) to reduce tiny topology errors. We then converted polygons to boundary lines (`st_boundary`) and noded the resulting line network so that shared boundaries were split into consistent, non-overlapping segments (using `st_node`). This produced a set of short border segments that collectively traced all HOLC polygon boundaries. Very small segments (under 5 meters) were removed.

To identify which HOLC polygons lay on each side of a given border segment, we buffered each segment by a small distance (10 meters, with a 25-meter fallback) and intersected the buffer with HOLC polygons. This intersection step assigned up to two adjacent HOLC polygons to each segment; segments with only one match were flagged as perimeter edges. Each segment was then labeled with the HOLC grade on both sides (e.g., grade A vs. grade D) and assigned a stable `border_id` based on the pair of adjacent polygon ID's (or NA for perimeter borders). Finally, we dissolved all segments sharing the same `border_id` to create one continuous border `polyline` per unique polygon pair, computed total border length in meters, and stored both the segment-level and dissolved border datasets.

E-3 Natural boundary designations

To measure whether HOLC neighborhood borders aligned up with major physical features, we link each HOLC border segment to nearby rivers and railroads. Starting with the map of HOLC polygons, we added three line-feature datasets: (i) a U.S. rivers and streams layer from Esri's ArcGIS Living Atlas, (ii) a small rivers layer built from an ArcGIS North America Rivers dataset and (iii) a historical railroads shapefile for 1826–1911 (Atack, 2016).

All layers were cleaned and put into the same projected coordinate system so that distances and lengths could be measured in meters. For each river and rail dataset, we buffered the line features by 200 meters and then intersected the buffer with the HOLC border segments (creation of which is described above). For each HOLC border, this gave the total number of meters of the border that falls close to a river or rail line as well as the share of the border's length that overlaps these buffered features. To streamline this process, we cropped the river and rail layers to the area around the HOLC borders and processed the overlays in geographic tiles, then combined results across tiles. Finally, we created simple indicators for whether each border is within the buffer distance of a river or rail line.